



hochschule mannheim

**Extension of two dimensions morphogenesis
simulation models of the urothelium into three
dimensions within the moduro simulation
environment**

Thorsten Mueller

Bachelor Thesis

for the acquisition of the academic degree Bachelor of Science (B.Sc.)

Course of Studies: Computer Science

Department of Computer Science

University of Applied Sciences Mannheim

11.11.2015

Tutors

Prof. Dr. Markus Gumbel, Hochschule Mannheim

Philipp Erben, Clinic of Urology, Medical Faculty Mannheim at the University of Heidelberg

Mueller, Thorsten:

Extension of two dimensions morphogenesis simulation models of the urothelium into three dimensions within the moduro simulation environment / Thorsten Mueller. –

Bachelor Thesis, Mannheim: University of Applied Sciences Mannheim, 2018. 59 pages.

Mueller, Thorsten:

Einsatz eines Flux-Kompensators für Zeitreisen mit einer maximalen Höchstgeschwindigkeit von WARP 7 / Thorsten Mueller. –

Bachelor-Thesis, Mannheim: Hochschule Mannheim, 2018. 59 Seiten.

Erklärung

Hiermit erkläre ich, dass ich die vorliegende Arbeit selbstständig verfasst und keine anderen als die angegebenen Quellen und Hilfsmittel benutzt habe.

Ich bin damit einverstanden, dass meine Arbeit veröffentlicht wird, d. h. dass die Arbeit elektronisch gespeichert, in andere Formate konvertiert, auf den Servern der Hochschule Mannheim öffentlich zugänglich gemacht und über das Internet verbreitet werden darf.

Mannheim, 11.11.2015

Thorsten Mueller

Abstract

Extension of two dimensions morphogenesis simulation models of the urothelium into three dimensions within the moduro simulation environment

The bladder is one of many organs in humans and animals. It is coated by the urothelium, which ensures that the bladder contains only urine. With bladder cancer the urothelium is not able to ensure its barrier function.

Bladder cancer is one of the most common cancer types in men. Cancer is able to spread into the surrounding organs and muscles. In the case of bladder cancer, the cancer arises in the urothelium and spreads then into the neighboring organs as it grows. If bladder cancer spreads into the surrounding organs and muscles the affected people have almost no chance of healing. Therefore, it is important to recognize bladder cancer early. To do so insights on how it arises are required. To receive these insights several simulations in two dimensions were done. With these simulations first insights of the rise of bladder cancer are revealed.

Because the urothelium is a three-dimensional product, the simulation should now be extended by a third dimension. With this extension it is hoped to receive new insights on how bladder cancer arises.

Contents

1	Introduction	1
1.1	Motivation	1
1.2	Background	3
1.2.1	Biology of the Urothelium	3
1.2.2	CompuCell3D	4
1.2.3	Glazier Graner Hogeweg Model	5
1.3	Objective	7
1.4	Outline	8
2	State of the Art	9
2.1	Moduro	9
2.2	Display and Simulation of the Urothelium	10
2.3	Moduro Toolbox	11
2.4	Proliferation models	11
2.4.1	Stem cells	12
2.4.2	Basal cells	12
2.4.3	Intermediate cells	12
2.5	Adhesion	13
2.6	Cell properties	13
2.7	Events in the simulation	13
2.7.1	Cell Growth	14
2.7.2	Mitosis	14
2.7.3	Necrosis	14
2.7.4	Mutation	14
2.7.5	Transformation	15
2.7.6	Urination	15
2.8	Fitness functions	15
2.8.1	Arrangement fitness function	15
2.8.2	Volume fitness function	16
2.8.3	Overall fitness function	17
2.9	3D functionalities	17
3	Methods	20
3.1	Lambda multipliers	20

3.2	Abstract methods	21
3.3	Calculation steps until urination	22
3.4	Amount of stem cells on the basal membrane	22
3.5	Adhesion Matrix	24
3.6	Target volume and target surface after mitosis	25
3.7	Approximation Error	25
3.8	Draw Sphere Cells	27
3.9	Growth of a sphere cell	31
3.10	Calculation of the volume and surface sites of a voxel sphere	32
4	Results	36
4.1	Structure of the program	36
4.2	Improvements of the program	36
4.2.1	Calculation of the amount of stem cells on the basal membrane	37
4.2.2	Monte Carlo Step (MCS) until the urination event	37
4.2.3	Target volume and target surface after mitosis	37
4.2.4	Conversion between the physical unit and the voxel unit	38
4.3	Draw sphere cells	38
4.4	Calculate the voxel volume and surface sites of a sphere cell	39
4.5	Grow sphere cells	40
4.6	Adhesion	40
4.7	Simulations	41
5	Discussion	48
5.1	Cell as a sphere	48
5.2	Adhesion	49
5.3	Voxel Density	50
5.4	Surface approximation	51
5.5	Surface Variation Pixels to Sphere	52
5.6	Simulation Results	54
5.7	CC3D	54
5.8	GGH Model	55
6	Future work	56
7	Conclusion	59
	List of Abbreviations	v
	List of Tables	vi
	List of Figures	vii
	Listings	viii
	Bibliography	ix

Chapter 1

Introduction

To start this paper a motivation for this scientific work is given. Then, the required knowledge is presented. After the presentation of the basic knowledge the objective of this bachelor thesis is displayed. To close this chapter an outline of this paper is given in the last section.

1.1 Motivation

One of several requirements regarding complex life is cell adhesion. If cells do not stick to each other the only living things would be cells. In humans and animals, organs and epithels are made of several cells and several layers of cells. This is also the case for the urothelium, which is an epithelium, i.e. a membranous tissue which consists of one or several layers. For the urothelium it is necessary that the cells stick to each other. Otherwise the functions of the urothelium could not be executed and also it would not be able to grow.

There are two types of tumors. One is the benign and the other one is the malignant tumor [1]. The benign tumor is self limited. Thus, it does not invade surrounding tissues nor does it spread into other body parts [1]. The malignant tumor on the other hand is not limited in its growth and is able to invade other body parts [1].

Since bladder cancer is one of the most common cancer types among men it is important to understand how and why the cancer is able to grow.

Bladder cancer starts to grow in the urothelium. With its growth and spread, the structure of cells sticking together changes. In this case, the urothelium is no longer

able to completely perform its tasks. In order to understand the urothelium, how and when bladder cancer appears, it is necessary to observe the epithel.

To understand the functionalities of organs and epithels, in general organisms, observations are essential. *For the urothelium this is already done, as there are several in vitro experiments about the methodology of the urothelium.* After an observation of an epithel or organ is complete, researches are able to predict how the observed organism will react in different situations. To verify these predictions a simulation is necessary. A simulation is an abstract illustration of the reality, but it can also be used to change reality in a for the research specific way, to get more knowledge of the epithel, or an organism in general.

A simulation should always be as simple as possible but also not too simple. Otherwise the simulation does not represent the reality. There are several programs with different algorithms for cell simulation. A popular algorithm is the Glazier-Graner-Hogeweg (GGH) model. This model is popular because it is easy to describe how cells interact with each other and it is possible to define constraints for the volume and surface of each cell.

The program CompuCell3D (CC3D) is a simulation program, which uses the GGH algorithm in its simulation. In the moduro project CC3D is used, and with the program the GGH algorithm is used.

The target of the moduro project is to predict under which circumstances bladder cancer occurs and when it is able to grow. Therefore, 16 different morphogenesis models of the urothelium were created. An overview of these models is displayed in table 2.1 at page 18. So far, all 16 models were simulated in 2D for a timespan of 720 days. The results reveal that some of the models are more realistic than others.

Because a cell is a three dimensional organism, a 2D simulation of the urothelium might not give as many aspects as a 3D simulation could do. Thus, the aim of this bachelor thesis is to create a 3D simulation of these 16 different models. With this 3D simulation it is hoped to receive new insights into the urothelium and how bladder cancer occurs.

1.2 Background

1.2.1 Biology of the Urothelium

Bladder cancer is the 4th most common cancer type in men according to everyday-health.com [2], every 36st out of 100.000 men gets it. Bladder cancer usually starts with some cells in the bladder growing uncontrolled. From these cells, the tumor can spread further into surrounding areas [3]. The most common bladder cancer type is the urothelial carcinoma [3].

The bladder is located in the lower urinary tract and consists of several parts. The urothelium is one part of it and coats the bladder [4]. More specifically, it covers the bladder from the renal pelvis to the proximal urethra [5], [6].

Two important tasks of the bladder are the storage and release of urine. To do so the bladder will extend, during the storage, and then shrink again [7]. One task of the urothelium is to form a distensible barrier [4], [8]–[11], which prevents unregulated exchange of ions, solutes, and toxic metabolites between the bladder and the blood [4], [8]–[10]. The urothelium ensures its barrier function, through enlargement and downsizing of its size. This is done by the largest cells of the urothelium, the umbrella cells. Since the umbrella cells are in direct contact with the bladder, it is their task to change size and form during the growth and shrink process of the bladder. Birdier [6] described the urothelium as “... a responsive structure capable of detecting physiological and chemical stimuli and releasing a number of signaling molecules.”. Another task of the urothelium is to control the movement and passage of macromolecules, ions, water, toxic metabolites and solutes [8], [9]. If the urothelium is damaged, it rapidly generates new cells, to ensure full functionality [5], [8], [9].

To receive a better overview of the different cell types, they are explained in the following paragraph. In figure 1.1 a simplified illustration of the urothelium with its different cell types and cell layers is provided.

The umbrella cells, also called superficial cells, are connected directly with the bladder and have an average diameter of 25 up to 250 μm [5], [9].

Below these cells the intermediate cells are located, with an average diameter of 10 up to 20 μm [5], [9]. There are at least three and up to five layers of the intermediate cells [9].

The smallest and the most common cells in the urothelium are the basal and stem cells. Those cells have a diameter of up to $10\text{ }\mu\text{m}$ [4], [9].

The urothelium consists of several layers. In the first layer, there are the basal and stem cells. Above them, there are several layers of intermediate cells. On top of the epithelium is one layer of umbrella cells.

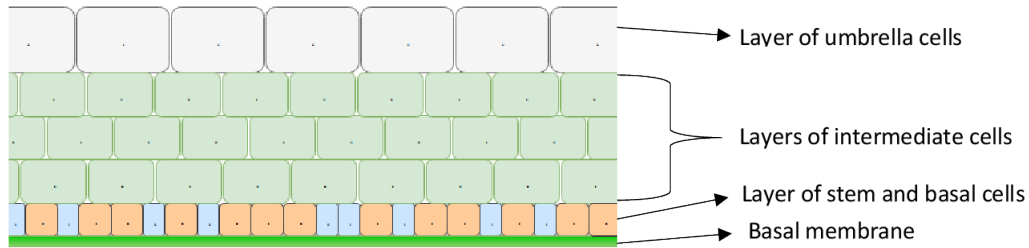


Figure 1.1: A simplified illustration of the urothelium. At the very bottom is the basal membrane. Above the membrane the stem and basal cells are displayed. The blue cells represent the stem cells, the red cells display the basal cells. Above the layer out of these two cell types, the urothelium contains several layers of intermediate cells. At the top of the urothelium is a layer of umbrella cells.

1.2.2 CompuCell3D

CC3D is an open-source program, which provides a simulation environment for multi- or single-cell-based modeling of tissues, organs and organisms [12]. To do so, CC3D uses the GGH model in its simulation. CC3D provides the possibility to create programs for the simulation, e.g. cell growth, mitosis, apoptosis or necrosis scripts, in Python, C++ or in CC3DML, which is their own Markup Language. With such programs CC3D allows the user to modify the behavior of the simulation for a specific purpose. CC3D uses the GGH approach, explained in the next section, section 1.2.3. It allows the user to choose between two cell-lattice types, i.e. a presentation of the pixels or voxels, a pixel with three dimensions, of a cell at a specific position in the simulation field. By default it uses a square-lattice of single pixels for each dimension, an example therefore is displayed in figure 1.2. CC3D provides the possibility to use a hexagonal-lattice, where the pixels are hexagons in two dimensions, or rhombic dodecahedrons in three dimensions. The core of a GGH simulation is the effective energy [13], CC3D tries to minimize this effective

energy every MCS, i.e. a calculation step in the simulation. The basic form for the effective energy is:

$$\mathcal{H}_{boundary} = \sum_{\vec{i}, \vec{j}} J(\tau(\sigma(\vec{i})), (\tau(\sigma(\vec{j}))) (1 - \delta(\sigma(\vec{i}), (\sigma(\vec{j}))) \quad (1.1)$$

This equation is a part of the equation of the GGH model. This model is explained in the next section. It is possible to extend this form in two ways. Either a volume or a surface constraint for each cell can be added. During each MCS an index-copy attempt takes place [13]. In this index-copy attempt a pixel is selected, and it is tried to overwrite a randomly chosen pixel, next to the current pixel. It succeeds and takes place if this index copy attempt decreases the effective energy [13]. Each MCS CC3D tries to minimize the effective energy with index copy attempts.

1	1	1	3	3	5	5	5
1	1	1	3	3	3	5	5
2	2	1	3	4	5	5	5
2	2	2	4	4	4	7	7
6	2	4	4	4	4	4	7
6	6	4	4	4	7	7	7
6	6	9	9	9	9	8	7
6	6	9	9	9	8	8	8

Figure 1.2: A square lattice in 2D. The same digits represent one cell $(\sigma(\vec{i}))$, whereas the different colors represent different cell types $\tau(\sigma)$.

1.2.3 Glazier Graner Hogeweg Model

Glazier and Graner developed several formulas and models which are presented in this subsection with focus on the Cellular Potts Model (CPM) and GGH model.

The GGH model is widely used in biological simulations, since it provides a good flexibility, extensibility and usability [14]. Glazier and Graner [14] developed the Extended Potts Model (EPM) as an extension of the large-q Potts model, which itself is an extension of the Ising Model. Nowadays, this model is called CPM [14]–[16]. Glazier and Graner extended the CPM in a way that also volume constraints

are considered for the hamiltonian, i.e. the effective energy, as it is displayed in the following equation:

$$\begin{aligned}\mathcal{H}_{CPM} = & \sum_{\vec{i}, \vec{j}} J(\tau(\sigma(\vec{i})), (\tau(\sigma(\vec{j}))) (1 - \delta(\sigma(\vec{i}), (\sigma(\vec{j}))) \\ & + \sum_{\sigma} \lambda_{vol} ((\tau)v(\sigma) - V_{target}(\tau(\sigma)))^2\end{aligned}\quad (1.2)$$

The hamiltonian of equation 1.2 describes the effective energy for the extension of the CPM model. The first sum describes J of all cells, the adhesion energy between different cells. Therefore, every cell has a specific cell type $\tau(\sigma)$ [15], [16]. Each cell is placed onto a lattice with a spin $(\sigma(\vec{i}))$ for every given dimension [14], [15]. The adhesion energy between cells is only considered if the kroenecker delta is 0. Thus, the adhesion energy between cells is considered if $\delta(\sigma, \sigma') = 0$ [14]–[19].

With the second sum over all cells the volume of each cell is now considered within the effective energy. The user is now able to set a target volume $V_{target}(\tau(\sigma))$ for each cell and a multiplier λ_{vol} for the deviation between the current volume $(\tau)v(\sigma)$ and the target volume. During the simulation this deviation is tried to be kept as small as possible for every cell in order to keep the effective energy as small as possible.

Together with Hogeweg Glazier and Graner further developed the created extension of the CPM. The further developed model is called GGH model. The main extension is that the user is now able to add surface area constraints [14]–[16] as well as to use a negative boundary energy [14]. With the surface constraint the equation for the effective energy of the GGH model is:

$$\begin{aligned}\mathcal{H}_{GGH} = & \sum_{\vec{i}, \vec{j}} J(\tau(\sigma(\vec{i})), (\tau(\sigma(\vec{j}))) (1 - \delta(\sigma(\vec{i}), (\sigma(\vec{j}))) \\ & + \sum_{\sigma} \lambda_{vol} (\tau)v(\sigma) - V_{target}(\tau(\sigma)))^2 \\ & + \sum_{\sigma} \lambda_{sur} (\tau)s(\sigma) - S_{target}(\tau(\sigma)))^2\end{aligned}\quad (1.3)$$

In addition to the hamiltonian of equation 1.2 is the surface constraint. It has the same principle as the volume constraint. Thus, the user is able to define a target surface $S_{target}(\tau(\sigma))$ for each cell and a multiplier λ_{sur} for the deviation between the target and the actual surface $(\tau)s(\sigma)$ of each cell. Since the volume and surface

constraint are included in the effective energy, it should be possible to use these two parts of the effective energy to shape the cells.

Beside the surface constraint the new model allows the user to model (a): cell growth and proliferation (b): mitosis, i.e. cell division (c): fields, forces and diffusion and (d): chemotaxis and haptotaxis [14].

Glazier et. al. describe their model as:

"GGH models define biological structure consisting of the configuration of a set of *generalized cells*, each represented on a *cell lattice* as a domain of lattice sites sharing the same cell index [...], a set of *internal cell states* for each cell [...], and a set of *auxiliary fields* ..." [14].

"Initial conditions emulating a particular biological configuration rather than random initial conditions." [14] brings the advantage that the GGH model now has biologically motivated properties instead of physically motivated properties [14].

1.3 Objective

The aim of this bachelor thesis is to create a 3D morphogenesis simulation of the urothelium using CC3D. Because the simulation models and the program for a 2D simulation are given and the simulation is done by CC3D, the task is to modify the current application, of the 2D simulation, in a way that this program can be used for a 3D simulation.

The required changes are all in the program, because the models of the 2D simulation should be also used for the 3D simulation. Therefore, some parts of the program have to be modified whereas other parts have to be developed. Because a third dimension will be added to the simulation, it is possible to try to let the cell have a different shape than in the 2D simulation. The result of this bachelor thesis will be presented with an analysis of an 3D simulation. A model therefor is selected out of the models which were created earlier in the project. These models are explained in section 2.4 at page 11.

1.4 Outline

Chapter 'State of the Art' provides the status at which the project was at the beginning of this bachelor thesis. Once the basic knowledge and the 'State of the Art' are explained, the modifications in the program during this journey are revealed in chapter 'Methods'. Then, in chapter 'Results', the outcome of this thesis is presented. After the results are presented, these are discussed of different perspectives in chapter 'Discussion'. In chapter 'Future Work' ideas for the future of the project are presented and to round up this paper a conclusion is provided in chapter 'Conclusion'.

Chapter 2

State of the Art

In this chapter informations about the current project are revealed. At the beginning the properties of the project are explained and later in this chapter the simulation program is presented. The sections 2.5 to 2.9 are explained based on the program of the project, whereas the other sections are presented based on previous work of the project.

2.1 Moduro

In the project moduro stands for 'Modeling of the Urothelium with the GGH approach'. The department of Medical Informatics at the University of Applied Sciences Mannheim and the Clinic of Urology in cooperation with the Medical Faculty Mannheim at the University of Heidelberg participate in this project. The aim is to predict how and when bladder cancer arises.

The current moduro project has a stable 2D simulation of 16 different models. The simulations are performed by CC3D. During the simulation statistics about the current simulation are written in text files and can be read out by the moduro toolbox. The project consists of a program and several models, both are written in Python. The models include properties of cell behavior. Therefore, the adhesion energy between cells and the possibilities of the new cell types after mitosis are defined in the different models. The application modifies the cell behavior, for instance it checks when a mitosis takes place and how fast the cell will grow.

2.2 Display and Simulation of the Urothelium

In the 2D simulation, the urothel is simulated with a size of $500\text{ }\mu\text{m}$ for the x-axis and $150\text{ }\mu\text{m}$ for the y-axis. Because the voxel density is 0.8, the size of the urothelium is represented with 400 pixels at the x-axis and 120 pixels at the y-axis. The voxel density describes how many pixels are used to display $1\text{ }\mu\text{m}$. CC3D allows the user to use any simulation size, as long as the required hardware is able to handle the simulation.

It is possible to use CC3D on several cores of the CPU. In the project one core for a simulation is used, because otherwise CC3D splits the simulation field into different grids. As a result race conditions can occur at the edges of these grids [13]. This means it is possible that a cell is in two grids. Thus, one half is in one grid and the other half is in another grid. During the simulation both grids would calculate the volume of the cell and both would apply the new volume of their calculation but it is not checked which result has to be used. Therefore, in order to reduce wrong results, it is necessary to avoid race conditions.

The 2D simulations of the urothelium cover a timespan of 720 days. In the simulations one day is split up into 500 MCS. Therefore, the simulation covers 360000 MCS. The simulation duration can be set in the program. Thus, the user defines how many MCS simulate one day and how long the simulation runs. At the first calculation step, MCS 0, the simulation is initialized. An illustration of an initial simulation is displayed in figure 2.1. Because morphogenesis is simulated, the urothelium is proposed to grow and to proliferate in the given area. An illustration therefor is presented in figure 2.2.

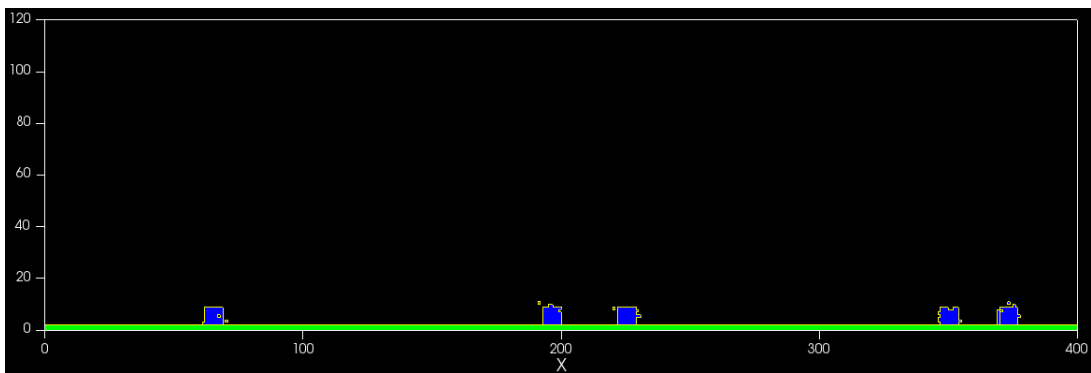


Figure 2.1: Initial state of a 2D simulation of the model SPA/BPCD/IPCD

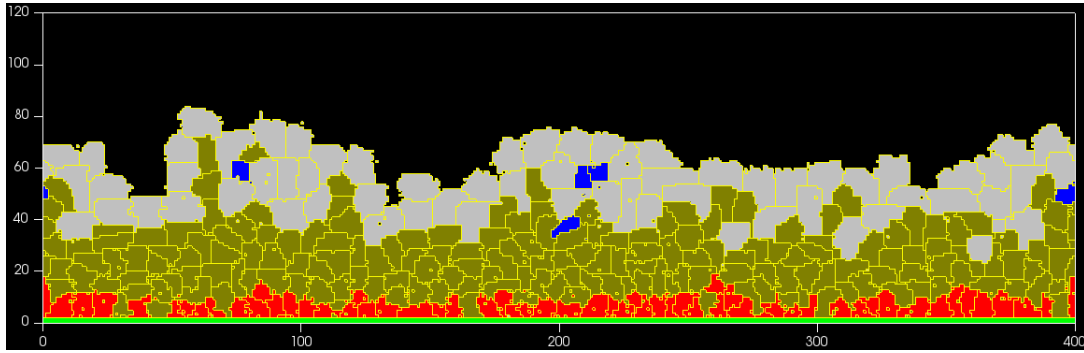


Figure 2.2: 2D Simulation of the model SPA/BPCD/IPCD after 33 days

2.3 Moduro Toolbox

The moduro toolbox is a software tool, which is able to visualize data in order to evaluate a simulation.

Every 12 hours the simulation is checked for its reality. This is done with the fitness functions of section 2.8. The results of these calculations are written in several text files, in a by CC3D created directory of the simulation. The amount of cells of the different cell types and the overall amount of cells is saved as well. The moduro toolbox is able to read out the data of the text files and then visualize these. This visualization is done with charts and with a table.

CC3D saves some screenshots, of the simulation field, during the simulation. With these screenshots the moduro toolbox is able to create a video out of these screenshots. To create the video an extra program has to be installed which the toolbox would use.

2.4 Proliferation models

The 2D simulation of the urothel provides 16 different models. These models differ in which cell types after the mitosis are created.

At the initialization of a simulation stem cells are created and drawn on the basal membrane. These stem cells grow and split into basal cell. The basal cells grow and split into intermediate cells. These intermediate cells grow and split into the umbrella cells. Therefore, for every proliferation model of the stem cells every model of the basal cells is used and for every model of the basal cells every model of the intermediate cells is used.

With these mitosis concepts there are 16 different models in the project. These

models were created by an earlier version of the project [20] and are displayed and summarized in table 2.1 at page 18. The different proliferation concepts are explained in the following subsections.

2.4.1 Stem cells

The stem cells are the first type of cells which undergo mitosis. One concept has the identifier 'SSD' and the other one is called 'SPA'. In the first model it is modeled that every time a stem cell divides there will be one stem and one basal cell. In the second model the stem cell has a probability of 90% that it will be one stem and one basal cell after mitosis. There is also the chance with a probability of 5% each, that after mitosis of a stem cell there are two stem cells or two basal cells.

2.4.2 Basal cells

For the mitosis of basal cells there are 4 different models. The mitosis model 'BSD' describes that each basal cell which undergoes mitosis will create one basal and one intermediate cell. The model 'BPA' describes that there is either a 5% chance that the basal cell will become two basal or it will become two intermediate cells. There is a 90% probability that the cell become one basal and one intermediate cell. The model 'BPCD', describes that always a basal cell becomes two basal cells during mitosis and if the basal cell is not on the basal membrane it transforms into an intermediate cell. The model 'BCD' has the behavior that a basal cell immediately transforms into an intermediate cell if it is not at the basal membrane.

2.4.3 Intermediate cells

There are two different models how intermediate cells split. One is the 'IPCD', therefor during mitosis an intermediate cell becomes two intermediate cells. Each MCS it is checked if there is a cell around the intermediate cell. If this is not the case it is transformed into an umbrella cell. The second model is the 'ICD'. In this concept, the transformation of intermediate cells into the umbrella cells only hap-

pens if the intermediate cell is not enclosed by other cells.

2.5 Adhesion

During morphogenesis the cells not only grow, they also sort themselves. For cell sorting there have to be different adhesion values, i.e. how strong two different cells are holding on each other. In the project this is done with a matrix, which is applied for every of the 16 models. Such a matrix was created in an earlier version of the project [20] and is displayed in table 2.2 at page 19.

2.6 Cell properties

In the project the physiological constraints of a cell are included. In an earlier version of the project these were evidenced [20] and are displayed in table 2.3 at page 19. In the program these constraints are converted into pixels and then applied.

In the simulation every cell has several attributes. Moreover, each cell has a cell dictionary, in which additional attributes are stored. The properties regarding the cell type are likely what every cell in general has, e.g. a min- max diameter, a min-max volume, growth in μm per day or the time until apoptosis, i.e. cell death.

The attributes in the cell dictionary are mainly used for decision making. Some values are the current and expected live time, a flag for necrosis and if a cell is inhibited, i.e. enclosed by other cells.

2.7 Events in the simulation

In the simulation program there are several events modeled. These events can occur every calculation step or at a specific MCS in the simulation.

The events which are performed every MCS, except for MCS 0 and every MCS of factor 250, are a) cell growth, b) the check for mitosis, c) cell death, d) cell transformation and e) cell mutation. The event which occurs every 12 hours, every

250 MCS, is f) urination. These events are presented in detail in the following subsections.

2.7.1 Cell Growth

In the project the maximum possible growth of a cell is calculated and applied. This calculation is used for the relation volume and target volume as well as for the relation surface, surface and target surface. Because the volume and the surface of a cell are calculated by CC3D and can only be read out, the target volume and target surface are calculated in the program and set.

2.7.2 Mitosis

The verification if a cell divides or grows further is done in every simulation step, except for these with a factor of 250. Therefore, it is possible to define a very specific calculation step at which a cell divides, as there are 500 MCS per day. In order that a cell divides it grows over its maximal size before it divides. The cells which are able to grow and as a result divide are a) stem cells b) basal cells and c) intermediate cells. The umbrella cells grow as well, but they do not split.

2.7.3 Necrosis

If a cell dies, necrosis takes place. In the program a flag in the cell dictionary is set. Every calculation step, the program checks if a cell dies or not. If so, the cell will shrink and as a result disappear.

2.7.4 Mutation

After 2 days, 1000 MCS, it is possible that a cell mutates, i.e. it becomes malignant. Each cell type has its own probability to become malignant. In the current simulation it is not considered that cells mutate since the probability for each cell type to mutate is 0% in the program.

If a cell mutates, there is also the flag for necrosis set. Thus, the cell shrinks and disappears.

2.7.5 Transformation

A transformation can take place if at least one intermediate cell is created. If the intermediate cell is not enclosed by other cells, it is transformed to an umbrella cell.

2.7.6 Urination

Every 12 hours, every 500 MCS, a urination takes place. The first urination event takes place at MCS 375. This is simulated in a way that randomly 2% of the cells in direct contact with the bladder are washed out. In the program a flag for necrosis is set and the cells will disappear because of the necrosis event.

2.8 Fitness functions

In order to validate the simulated models, there are several functionalities which check if the model is realistic or not. These functions check every 12 hours, every 250 MCS, if the model is realistic or not. The results of these fitness functions are written into several files, and can be read out by the moduro toolbox.

2.8.1 Arrangement fitness function

The arrangement fitness function ensures that the strata of the simulated urothelium has the correct order [20], i.e. that the first layer on the basal membrane consists only of stem and basal cells **REFS** the next three to five layers consists only of intermediate cells **REFS** and that there is one layer of umbrella cells **REFS**

$$lib = \frac{L - lib}{L} \quad (2.1)$$

$$f_A = 1 - \frac{((1 - L_B) + (1 - L_U) + lib + (1 - L_O))}{4} \quad (2.2)$$

In equation 2.1 L refers to the amount of layers in the urothelium. lib describes the amount of layers between the stem and basal cell layer and the umbrella cell layer at the top of the urothelium, which include not only intermediate cells. Thus, if the layers between the first and last layer consist only of intermediate cells, the equation 2.1 has the result 0.

In equation 2.2 L_B and L_U are boolean values, i.e. they have the value 0 or 1 and represent a false or true value. They are 1 if the first layer of cells consists only of basal or stem cells and if the most upper layer consists only of umbrella cells, otherwise they will be 0. lib is calculated in equation 2.1. L_O presents the optimum amount of layers. It is 1, if the amount of layers in the simulated urothelium is between 3 and 7, otherwise it is 0. The result of equation 2.2 is between 0 and 1, where 0 refers to a chaotic grown urothel with no reality in its structure and 1 refers to a perfectly structured urothelium.

2.8.2 Volume fitness function

This function calculates the relative volume regarding the current volume of the different cell types in the urothel. The relative amount of the different cell types should be: stem and basal cells = 10%, intermediate cells = 67% and umbrella cells = 23% considering an average thickness of 85 μm [20]. Therefore the formula is:

$$f_{V_i} = \frac{1}{4\left(\frac{V_{Si} - V_{Ii}}{V_{Si}}\right)^2 + 1} \quad (2.3)$$

V_{Si} and V_{Ii} describe the should and the actual is volume of a specific cell type i [20]. This calculation is done three times. One time for the stem and basal cells, one time for the intermediate cells and one time for the umbrella cells. The results of the three calculations are then further used to determine the relative volume overall.

$$f_V = \frac{f_{V_B} + f_{V_I} + f_{V_U}}{3} \quad (2.4)$$

In equation 2.4 f_{V_B} refers to the relative volume of the stem and basal cells, f_{V_I} presents the relative volume of the intermediate cells and f_{V_U} includes the relative volume of the umbrella cells.

The result of all four calculations, three times the equation 2.3 for every layer and

one time equation 2.4 is calculated and written into a text file and can be read out by the moduro toolbox later.

2.8.3 Overall fitness function

The ideas and equations of this subsections are found in the paper created earlier in the project [20].

The overall fitness function calculates the total fitness out of the volume and the arrangement fitness function. Therefore the average of both functions is calculated. For every calculation step, the arrangement and volume fitness function are calculated and the overall fitness is calculated. Therefore the formula is:

$$f(t_i) = \frac{f_V(t_i) + f_A(t_i)}{2} \quad (2.5)$$

t_i describes a specific point of time, in MCS, at which this calculation is done. At the end of the simulation the average of the overall fitness function is calculated to determine the reality of this simulation. Therefore, the formula is:

$$f = \frac{1}{e + 1} + \sum_{i=0}^e f(t_i) \quad (2.6)$$

The result of the calculation is between 0 and 1. Where 0 describes no reality at all and 1 presents a perfect realistic simulated urothelium.

2.9 3D functionalities

The functionalities of the program are able to be used in 3D. Whenever a part of the program is required to be used in 2D as well as in 3D, it is checked if the simulation field has a third dimension or not. Examples for such functionalities are the fitness functions of the section before or the decision how many stem cells are placed on the basal membrane, which is modified and explained in section 3.4.

Because so far only the 2D simulations were progressed, it is important to keep the functionalities of the 2D simulation in the program. Doing so it is possible to switch between a 3D and a 2D simulation, as well as the benefits of both simulation types can be observed.

Table 2.1: 16 different models derived in an earlier version of the project [20] as there are different ways of proliferation and mitosis are simulated for the different cell types. S refers to the stem cell whereas B displays a basal cell. I presents the intermediate cell and U refers to the umbrella cell. BM displays the basal membrane and M presents the Medium cell type, which is a by CC3D specific cell type.

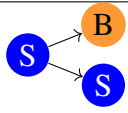
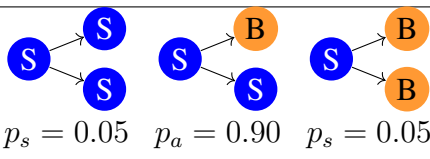
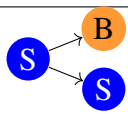
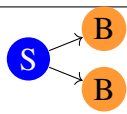
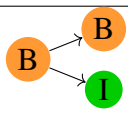
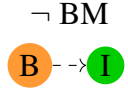
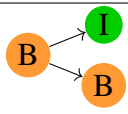
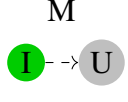
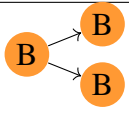
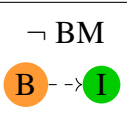
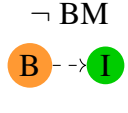
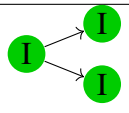
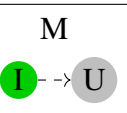
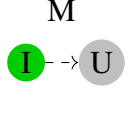
Type	ID	Description	Model
Stem cells	SSD	Stem cell-like division	
	SPA	Stem cell population asymmetry	 $p_s = 0.05$  $p_a = 0.90$  $p_s = 0.05$
Basal cells	BSD	Stem cell-like division in basal cell	
	BPA	Basal cell population asymmetry	 $p_s = 0.05$  $p_a = 0.90$  $p_s = 0.05$
	BPCD	Proliferation and contact differentiation of basal cells	 and  $\neg \text{BM}$
	BCD	Only contact differentiation of basal cells	 $\neg \text{BM}$
Intermediate cells	IPCD	Proliferation and contact differentiation of intermediate cells	 and  M
	ICD	Only contact differentiation of intermediate cells	 M

Table 2.2: Adhesion matrix for a model in the simulation. Smaller values refer to more adhesion and higher values mean less adhesion. The cell type M is the medium cell type, it is by CC3D a specific cell type which is everywhere in the available space in the simulation, and BM is the basal membrane. This table was created in an earlier version of the project [20].








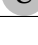




Types		M	BM				
Medium	M	0	14	14	14	14	4
Basal membrane	BM		-1	1	3	12	12
Stem cell				6	4	8	14
Basal cell					5	8	12
Intermediate cell						6	4
Umbrella cell							2

Table 2.3: Constraints of the different cell types. Volumes V in μm^3 , diameters d in μm . The 'Volume' and 'Surface' column describe how the λ_{vol} and the λ_{sur} should be set for each cell type. This table was created in an earlier version of the project [20].

Cell type		V_{min}	d_{min}	V_{max}	d_{max}	Volume	Surface
Stem		268	8	523	10	perfect	average
Basal		381	9	523	10	important	average
Intermediate		905	12	1767	15	important	poor
Umbrella		1767	15	3591	19	important	poor

Chapter 3

Methods

This section gives an overview over all changes in the project which were done during this bachelor thesis. These changes include some small improvements of the application as well as the approach to draw a sphere cell. First minor changes are described briefly, further onwards in this chapter the more complex changes are explained.

3.1 Lambda multipliers

In the project the multipliers λ_{vol} and λ_{sur} are set if a cell is initialized. λ_{vol} is set a second time in the necrosis event, if the program models that a cell dies.

In each cell object, there were two additional multipliers, one for the surface and one for the volume constraints. Because these values are not used in the program and they do not influence or set the λ_{vol} or λ_{sur} which CC3D uses, these two values were deleted. Moreover, in one place there were methods to calculate the lambda values. Because these methods are not used in the project and they had a multiplier itself to calculate the multiplier for the specific part of the effective energy, they were deleted as well.

In the project the multipliers λ_{vol} and λ_{sur} are now set each time when a cell is initialized. A second time the multiplier λ_{vol} is set, if necrosis takes place. Now the unnecessary methods and values for the multipliers values are removed. Thus, no confusion about which constraint values in the program are used arises.

3.2 Abstract methods

The program has several classes with methods which were not used because of polymorphism. Polymorphism is a method out of Object Oriented Programming (OOP). Another technique of OOP is the use of abstract classes and abstract methods. To explain polymorphism, abstract classes or abstract methods in detail, would take too much space out of this bachelor thesis. Thus, the change in the program is explained in the following paragraph.

In the project are several classes which inherit from each other. In these classes were the same methods implemented. It is not required that several classes have the same methods. Such methods are redundant methods, as long as they do not differ in their functionality. For these methods it is possible to declare them as an abstract method. An abstract method contains only the method construct, but no functionality. Due to polymorphism the class in which such an abstract method is implemented is used to call the method of the class in which the method is implemented, if one of the two class inherits from the other class.

For Python the library 'ABC' exists. ABC is a shortcut and stands for Abstract Bases Classes. With this library it is possible to declare an abstract method. To do so every class with one or more abstract methods needs to initialize a special variable. With this variable Python is able to recognize that there are abstract methods included.

Listing 3.1 displays how the variable has to be initialized in order that abstract methods are recognized. Listing 3.2 is an example for an abstract method in Python. If a class has at least one abstract method, it is an abstract class. In Python abstract classes can include implemented methods as well as abstract methods.

```
class ModelConfig(object):  
    __metaclass__ = ABCMeta
```

Listing 3.1: The initialization of a class variable which is required by Python in order to detect abstract methods and abstract classes.

```
@abstractmethod  
def _createExecConfig(self):  
    pass
```

Listing 3.2: Declaration of an abstract method.

Using abstract methods creates more structure and clarity within the project. Therefore, the abstract declarations in this project created a much better clarity of the structure of the project and of the methods, which were used in the classes.

3.3 Calculation steps until urination

To simulate the urination in the program it was checked if the current calculation step is larger than 250 and a factor of 125. Every 250 MCS the volume- and arrangement fitness functions are calculated and no other events in the simulation take place. Therefore, the urination was simulated every twelf hours. The check if the current MCS is a factor of 125 happens through the modulo operator. Thus, the current calculation step is divided by 125 and if the remainder of the result, as a whole number, is 0 it is a factor of 125.

The check when the urination event takes place is modified. This modification took place because in an earlier version of the project it was evidenced that the urination should take place every six hours [20], but within the code it took place every twelf hours. The urination event now takes place if the current calculation step is larger than 250 and if the current MCS modulo 125 equals 1. Therefore, the urination event is used every six hours, at MCS 376, 501, 626, 751, etc..

3.4 Amount of stem cells on the basal membrane

In an earlier version of the project it was evidenced that around 12% of the area of the basal membrane are required to be filled with stem cells in order to have an optimal proliferation during the morphogenesis of the cells [20]. In the project the calculation of the amount of stem cells for two dimensions were correct but it was incorrect for three dimensions. Moreover, one factor was calculated out of the diameter of the stem cells. This factor stayed the same for all sizes of the simulation fields.

Because the basal membrane in a 2D simulation is only displayed at the x-axis and at a 3D simulation it is displayed with the x- and z-axis, the calculation for two dimensions considers the x-axis and the calculation for three dimensions considers the x- and z-axis. Therefore, in two dimensions the area of the stem cells should be calculated by using the cell diameter. An illustration therefor is displayed in figure 3.1. For a 3D simulation it is possible to calculate the area of stem cells with a circle with the formula $A = \pi \cdot r^2$, because the y-axis is not considered in this calculation. The area of a circle is also used to determine the amount of stem cells on the basal membrane. An example for the basal membrane and a stem cell in three dimensions is displayed in figure 3.2.

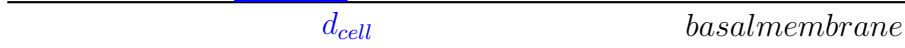


Figure 3.1: Considered area to spread the stem cells in 2D with an example of one stem cell placed on the basal membrane. Because only the x-axis is considered the diameter of a cell is used for the calculation

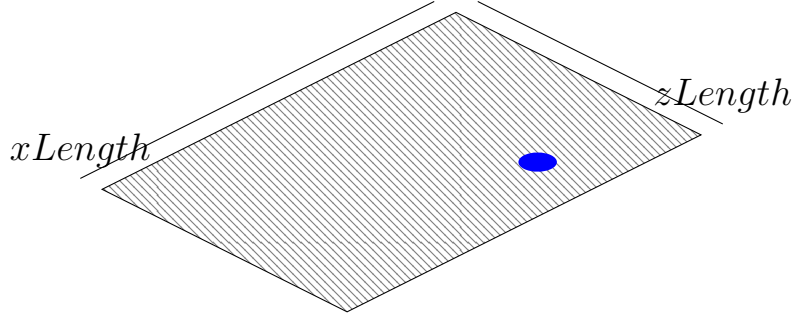


Figure 3.2: Considered area to spread the stem cells in 3D with an example of one stem cell placed on the basal membrane. The hatched area displays the basal membrane and the circle represents one stem cell.

With equations 3.1 and 3.2 it is possible to calculate the amount of stem cells in two dimensions. $A_{stemcells}$ refers to the area at the basal membrane which can be used for stem cells. c is a constant, which describes 12% of an object. Thus, $c = 0.12$. $xLength$ presents the length of the x-axis and $zLength$ includes the length of the z-axis of the basal membrane, d_{cell} describes the diameter of the cell and $Amount_{StemCells}$ describes the amount of stem cells at the basal membrane.

$$A_{stemcells} = xLength \cdot c \quad (3.1)$$

$$Amount_{StemCells} = \frac{A_{stemcells}}{d_{cell}} \quad (3.2)$$

Equation 3.1 ensures that only 12% of the given area is used. Formula 3.2 then calculates the amount of stem cells on this given area. Because the result of the calculation is often not a whole number, as last step the result is checked if the first decimal digit is larger or equal than 5 and then it is rounded up.

As table 3.1 and 3.2 at page 23 and 27 display, it is important to round the result. Otherwise there would be an approximation error and as a result a calculation error. For three dimensions equation 3.1 has to be extended. An illustration therefor is figure 3.2. Equation 3.2 has to be modified, because the area of a circle, instead of

Table 3.1: Possible approximation error by not rounding the result of equation 3.2. The first column describes the length of the basal membrane, the values are in μm . In the second column the result of equation 3.2 is displayed. In the third column the result of the second column is rounded up in the first row. In the second row this result is casted. The fourth column displays how much space the stem cells, in μm , of the rounded or casted result of equation 3.2 require. The last column displays the physical space required in percentage to the basal membrane.

xLength of the basal membrane	Result of equation 3.2	Amount of stem cells	Area used of stem cells in μm	relative used area
200	~ 2.66	3	27	13.5%
200	~ 2.66	2	18	9%

the diameter, is used for the calculation. Therefore, equations 3.3 and 3.4 are used to calculate the amount of stem cells in three dimensions.

$$A_{stemcells} = (xLength \cdot zLength) \cdot c \quad (3.3)$$

$$Amount_{StemCells} = \frac{A_{stemcells}}{\pi \cdot r^2} \quad (3.4)$$

The result of formula 3.4 has to be rounded as well, otherwise the program would include rounding errors. These calculations are now included in the program.

3.5 Adhesion Matrix

To have a realistic simulation it is necessary to have a correct adhesion matrix. The matrix which was used for the 2D simulation is displayed in 2.2 at page 19. It might be that the adhesion values are useful for the 2D simulation but not for the 3D simulations. Therefore, observations of different adhesion values between different cell types are done and explained in the following.

To find the correct adhesion values, the simulation program was modified in a way that two cells in a small simulation field are placed next to each other. As a first step, the cells were touching each other at MCS 0. Then, they were observed during their growth process. The different observations were saved. In the second step, the two cells were placed with some distance to each other and it was observed how they behave as they touch during their growth process for different adhesion values.

With the observations of both techniques a new adhesion matrix for the different cell types was created. This adhesion matrix is displayed in table 4.1 at page 41.

3.6 Target volume and target surface after mitosis

Mitosis of the cell is simulated by CC3D. In the simulation mitosis is simulated as the following: one cell splits into two cells. The cell which splits dies and then two new cells out of the dead cell are created.

In the program it is specified and checked if and when a cell splits. CC3D decides where the cell splits and calculates the volume and surface of the two new cells. In the program attributes of the new cells, e.g. the target volume or the target surface, are calculate and set.

The target volume were calculated by dividing the target volume of the cell before mitosis by two. This value is applied for both new created cells. The problem with this technique is that it is possible that the cell might not split in the middle. In the case of mitosis, setting the target volume of the two created cells without the knowledge of the current volume is a source of error. Because the target volume of the two new cells was set without considering the current volume of the cell, it occurred that one of the new cells, after mitosis, had a target volume which was smaller than the current volume.

After mitosis both cells are initialized. Thus, the target volume and target surface are calculated and set. After the initialization of the cells, the target volume of the new cells were set to the target volume of the cell before mitosis divided by two.

Because the target volume is calculated out of the volume of the cell during the initialization process, the calculation of the target volume is removed out of the mitosis event. Now the target volume and target surface after mitosis is set only during the initialization process of the new cells.

Now, the target volume and target surface after mitosis is calculated and set dependent on the by CC3D given volume.

3.7 Approximation Error

The project includes conversions from μm into voxels. In CC3D the amount of pixels and voxels, e.g. for the surface of a cell, has to be set as data type integer, i.e.

a whole number. Therefore, it is possible that in some places in the program there are calculation errors during a conversion of the units. In the project, the values of unit μm are saved with the data type float, i.e. a number with decimal digits. To set these values as a whole number the values are casted, i.e. the decimal digits are cut off, into the data type integer as it is described below.

Whenever a conversion from μm into voxels is done the complete calculation is calculated with decimal digits. After the calculation is done it is verified if the first decimal digit is larger or equal to 5. If this condition is true the result is increased by 1, otherwise not. As a last step the result is casted. This technique has the advantage that calculation errors due to casting are removed, because the cast is the very last step. It is possible that the program still includes some rounding errors, but these can not be removed because CC3D requires the amount of voxels as a whole number and the calculations are done with decimal digits.

In listing 3.3 below, the cast and the rounding of the result are done in the last step of the calculation.

```
def calcVoxelVolumeFromVolume(self, volume):
    r = (3 * volume / (4.0 * PI)) ** (1.0 / 3.0) # Radius of a sphere with
        known volume.
    rDimension = r * self.voxelDensity
    if self.dimensions == 2:
        return int(self.__truncate(PI * (rDimension ** 2))) # Area of a circle.
    else:
        result = 4.0 / 3.0 * PI * (rDimension ** 3)
        if result % 1.0 >= 0.5:
            result += 1

    return int(result)
```

Listing 3.3: Function to calculate the volume of a sphere in voxels out of a given physical volume. First out of the given physical volume the radius is calculated. Then it is converted into the voxel unit. Next the volume of the voxel sphere is calculated and as last step the result is rounded and casted.

One purpose of the displayed function is to calculate the voxel volume out of the physical volume of a cell. In the simulation a minimum and a maximum volume for each cell type is calculated. These values are used in the calculation to determine if mitosis takes place or not.

For the basal cell the minimum volume is $381\mu\text{m}$ and the maximal volume is $523\mu\text{m}$. In table 2.3 at page 19 the constraints of the different cell types in μm are displayed. In table 3.2 three different possible calculations of the conversion of a volume in μm into a volume in voxels are presented.

Table 3.2: Three different ways to calculate the voxel volume out of a given physical volume. The first column describes the physical volume in μm . In the second column the radius in μm out of the volume is calculated. Next, the radius is used as it is, casted or rounded up. In the fourth column the exact result of the volume in voxel is presented and in the last column the rounded result of the voxel volume is displayed.

Volume in μm	radius in μm	radius used in further calculation	not rounded result in vx	rounded result in vx
381	4.49	4.497	1285.67	1286
381	4.49	4	904.77	905
381	4.49	5	1767.15	1767

In the table, the first row calculates the voxel volume as it is done in this thesis. Thus, rounding and casting is the last step in the calculation. In the second row the radius is calculated and casted. Then this casted radius is used for the further calculation. The third row calculates the radius and rounds it immediately. This rounded radius is then used for the further calculation.

As the table displays, there is a significant difference in all three results. Because such a calculation is used to determine when a cell splits as well as it calculates the growth per MCS, it influences the result of a simulation. Thus, it is important to round and cast the result as very last step in the calculation.

3.8 Draw Sphere Cells

Because a cell as a sphere is an approximation to a cell in the urothelium, it is a possible technique to draw and further simulate a cell as a sphere.

To be able to draw a sphere out of voxels it is required that a cuboid lays around the sphere, as it is displayed in figure 3.3. The cuboid has to be at least as large as $2 \cdot \text{radius}$ of the sphere. In addition, the cuboid should not be larger than necessary, otherwise there would be unnecessary computable cost. The illustration in figure 3.4 at page 30 display the perfect size of a square and a circle. These 2D objects are chosen to display the boundaries of a circle in a square as well as the boundaries would be in three dimensions.

To be able to draw a cell as a sphere, CC3D has to allow the user to draw several different voxels in the simulation field, all containing one cell. Since CC3D allows

the user to draw several pixels containing one cell, a solution for this problem is possible.

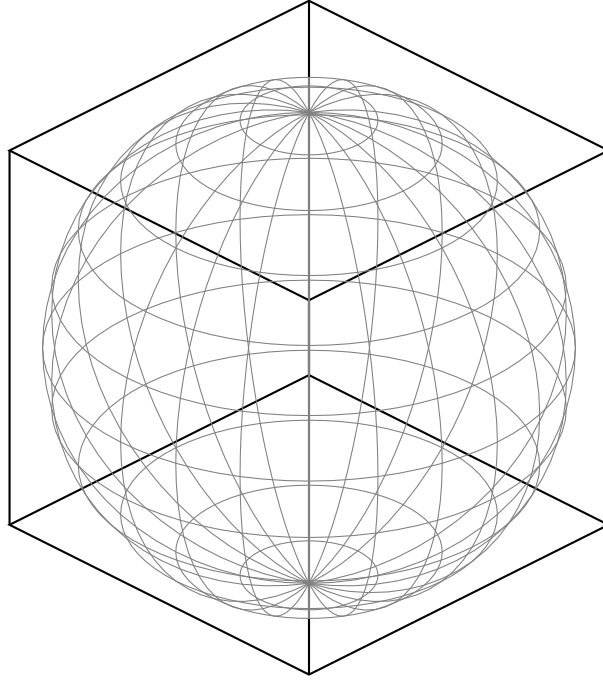


Figure 3.3: A cuboid layed around a sphere

Because the square lattice is used, the cuboid is filled with voxels. To be able to calculate every point within the sphere, the cuboid and the sphere are required to have the same center **REF** In this case equation 3.5 provides a mechanism in which every point within the sphere can be calculated.

$$\sqrt{(x_r - x_0)^2 + (y_r - y_0)^2 + (z_r - z_0)^2} \leq radius \quad (3.5)$$

In equation 3.5 x_r , y_r and z_r describe the current point of each of the three axis and x_0 , y_0 and z_0 describe the center of the sphere and cuboid. If the distance of the current x, y, z coordinate is smaller or equal to the radius the current point is within the sphere, otherwise it is outside of the sphere. Because a voxel itself contains several points, this equation, in this case with cuboids, has the weakness that only one point is considered. Thus, only one point of the voxel is considered in the decision whether the complete voxel is within the sphere or not. Since every voxel is a cuboid itself, the length of all corners are the same. This fact can be used to increase the accuracy of the equation above.

In the program it is possible to calculate the corner length of a voxel. Thus, it is possible to decide if the center of a voxel is at the inside or outside of a sphere. How the center of a voxel is calculated is explained in the following paragraph. Because the radius of the sphere is known, whether it is known or it is calculated out of the volume or the area of a sphere, the diameter of the cuboid can be calculated. Moreover, the voxel density is known in the simulation, the corner length of each voxel can be calculated as it is displayed in equation 3.6.

$$c = \frac{2 \cdot radius}{voxeldensity} \quad (3.6)$$

In equation 3.6 c describes the corner length of a voxel. With this corner length it is now possible to calculate the center of a voxel and use this center further to decide if the voxel is inside or outside of the sphere. To determine the center of a voxel the calculation has to be done for every of the three axes. The following three formulas display such calculations.

$$\begin{aligned} x_c &= x_r + \frac{x_{r+c} - x_r}{2} \\ y_c &= y_r + \frac{y_{r+c} - y_r}{2} \\ z_c &= z_r + \frac{z_{r+c} - z_r}{2} \end{aligned} \quad (3.7)$$

In equation 3.7 x_r , y_r and z_r describe the start point and x_{r+c} , y_{r+c} and z_{r+c} describe the end point of the voxel. With the calculations of equation 3.7 it is now possible to consider the center of a voxel in the decision if the voxel is in- or outside the sphere, as it is displayed in equation 3.8.

$$\sqrt{((x_c - x_0)^2 + (y_c - y_0)^2 + (z_c - z_0)^2)} \leq radius \quad (3.8)$$

To depict a cell as a sphere a new function had to be created. This function is named `addSphereCell` as it is displayed below in listing 3.4. In the method all required points, the start- and end points as well as the centers, of all three axis are given in μm . Thus, these points as well as the radius, which is also given to the function, and the step-length, i.e. the corner length of a voxel, are converted into the voxel unit. With all necessary points in the voxel unit it is now possible to iterate over all three axis and check for every voxel, if it is included in the sphere or not.

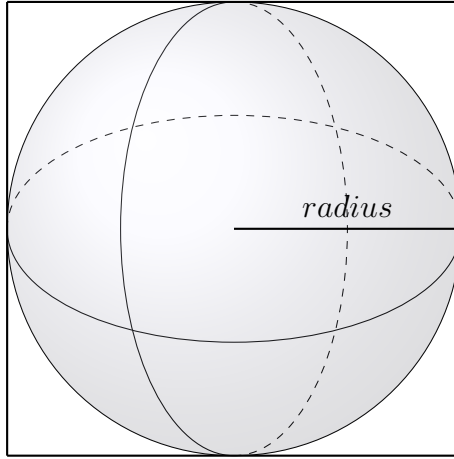


Figure 3.4: A cuboid with minimal size layed around a sphere

```
def _addSphereCell(self, typename, xPos, yPos, zPos, radius, steppable):

    cell = steppable.newCell(typename)
    xStart = self.execConfig.calcPixelFromMuMeter(xPos - radius)
    x0 = self.execConfig.calcPixelFromMuMeter(xPos)
    xEnd = self.execConfig.calcPixelFromMuMeter(xPos + radius)
    yStart = self.execConfig.calcPixelFromMuMeter(yPos - radius)
    y0 = self.execConfig.calcPixelFromMuMeter(yPos)
    yEnd = self.execConfig.calcPixelFromMuMeter(yPos + radius)
    zStart = self.execConfig.calcPixelFromMuMeter(zPos - radius)
    z0 = self.execConfig.calcPixelFromMuMeter(zPos)
    zEnd = self.execConfig.calcPixelFromMuMeter(zPos + radius)

    radiusPx = self.execConfig.calcFloatPixel(radius)
    stepLength = self.execConfig.calcFloatPixel(1)

    # loop over the center of each pixel to determine boundaries of the circle
    for xr in xrange(xStart, xEnd):
        for yr in xrange(yStart, yEnd):
            for zr in xrange(zStart, zEnd):
                rd = sqrt(
                    ((xr+((xr+stepLength) - xr)/2.)) - x0) ** 2 +
                    ((yr+((yr+stepLength) - yr)/2.)) - y0) ** 2 +
                    ((zr+((zr+stepLength) - zr)/2.)) - z0) ** 2)
                if (rd <= radiusPx):
                    steppable.cellField[xr, yr, zr] = cell
```

Listing 3.4: Function to draw a cell as a sphere. First all required points for the calculation are converted into the voxel unit. Then it is iterated over each of the three axis. During these iterations for each voxel the distance to the center of the cuboid and sphere is calculated and then it is checked if the voxel is within the sphere or not. If the voxel is a part of the sphere it will be added to the sphere.

To draw the cell as a sphere is the first step to have sphere cells in the simulation. Because it is possible to draw a cell as a sphere, the cells are considered in the rest of the paper as sphere cell.

3.9 Growth of a sphere cell

The simulation of the morphogenesis of the urothelium requires the growth of cells. Ideally the cells keep their shape, which they become as they are depicted.

In the simulation the current volume and surface of a cell is calculated by CC3D. Every user is able to influence these values by setting the target volume and target surface and the proper multiplier, λ_{vol} and λ_{sur} , for the specific part of the effective energy. As the goal of the simulation is to minimize the effective energy, the cell will change the current volume and surface in the direction of the set target volume and target surface.

To model the growth of a cell, the growth per day of the volume for the different cell types is set. Each calculation step the growth of one MCS is calculated and applied, 500 calculations steps are one day. After the growth of the volume is calculated and set as new target volume of the specific cell, a new target surface depending on the target volume is calculated and set.

In the program the target surface is calculated out of a real sphere and then multiplied by a factor. Because the surface of a sphere of voxels is larger than the surface of a real sphere, it is necessary to find the correct factor, by which the surface of a sphere has to be multiplied. This is necessary, in order to calculate the surface of a sphere of voxels.

For simplicity reasons, a first approximation of the factor is calculated in 2D. Thus, a circle and a square filled with pixels are used. An example therefor is displayed in figure 3.5 at page 33.

Figure 3.6 at page 33 displays an approximation, with which it is possible to calculate the factor for the surface.

In figure 3.6 the left square is considered as a pixel, it could be any pixel of the figure 3.5 through which the circle is included. Thus, the sides of the square are the same. The blue line represents the circle, in a way it could go through the pixel. A possible approximation is to insert a diagonal line. With this diagonal line an isosceles, right angular triangle is created as it is displayed at the right side of figure

3.6.

The following formula provides a way to calculate the sides of this triangle.

$$c^2 = 2 \cdot a^2 \quad (3.9)$$

The formula of equation 3.9 can be used to calculate the side a , as it is displayed in the following equation.

$$\begin{aligned} a &= \sqrt{\frac{c^2}{2}} \\ a &= \frac{c}{\sqrt{2}} \end{aligned} \quad (3.10)$$

Since the surface of a pixel has two corner sides, the equation to calculate the surface of a pixel sphere is

$$\begin{aligned} S &= 2a \\ S &= c \cdot \sqrt{2} \end{aligned} \quad (3.11)$$

This formula applies to all pixels, which are at the surface of the pixel sphere, c is considered as the surface of the circle. Thus $c = \pi \cdot r^2$.

The calculated factor $\sqrt{2}$ was tested for a sphere surface. Because this is an approximation to the surface of a pixel sphere, the tenth parts beside this factor are also tested mathematically. As figure 3.7 at page 34 displays the approximation with factor $\sqrt{2}$ still has some deviation. Almost no deviation between the surface of a sphere and a surface of a sphere of voxels appeared with a factor of 1.5. Thus, this factor is applied in the calculation of the target surface.

3.10 Calculation of the volume and surface sites of a voxel sphere

In order to determine the voxel volume and the surface sites of a sphere cell without the start of a simulation, an algorithm for this problem was created. Otherwise a new simulation in CC3D had to be started for every measurement of the volume and surface of the sphere cells.

Because a sphere and a cuboid are both symmetrical, it is possible to split both into

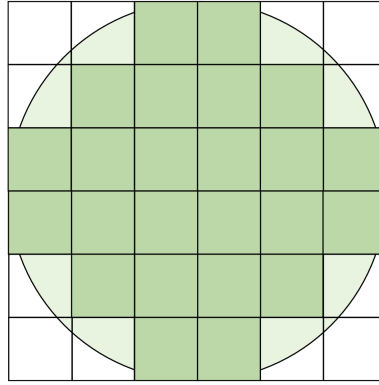


Figure 3.5: A circle in a possible pixel presentation. All small squares present pixels. The colored squares present the pixels, which are included in the pixel presentation of the circle.

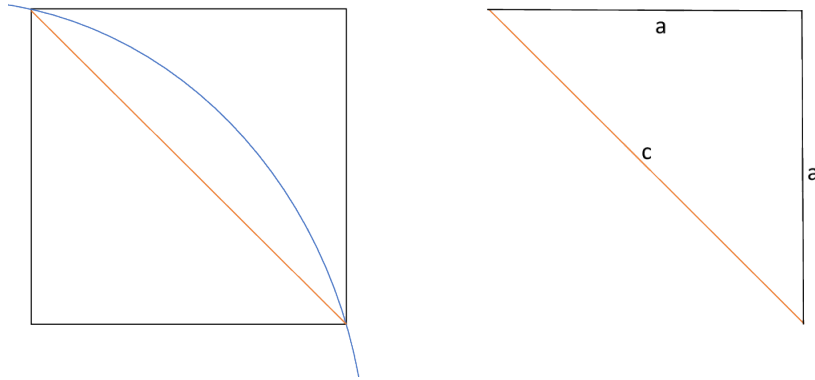


Figure 3.6: The left part of the illustration displays a pixel at the surface, in which the circle goes through. The blue line represents the circle. As an approximation to the surface line a diagonal line in the square is drawn. With this diagonal line an isosceles, right angular triangle appears and it is possible to calculate the additional surface of one pixel. This isosceles, right angular triangle is displayed at the right side of this figure.

eight pieces. Doing so only one eighth of the cuboid has to be calculated in order to determine the volume and the surface of the sphere. An example therefore is displayed in figure 3.8 at page 35.

To calculate which voxels are in the voxel sphere, the algorithm creates a x, z, y matrix. In the following calculations and decisions the center of each voxel is used. For every x, z coordinate in the eighth of the cuboid the y constraint of the circle is calculated. Next, every voxel at the x, z coordinate is checked if the center of the voxel is within this constraint or not. Thus, every voxel at a x, z coordinate gets checked if its center is within the sphere or not. This process is repeated until every x, z coordinate of the eighth of the cuboid is calculated. Every time a voxel is within the sphere, it will be marked with a 0 in the matrix. An example matrix is displayed in table 3.3 at page 35.

3 Methods

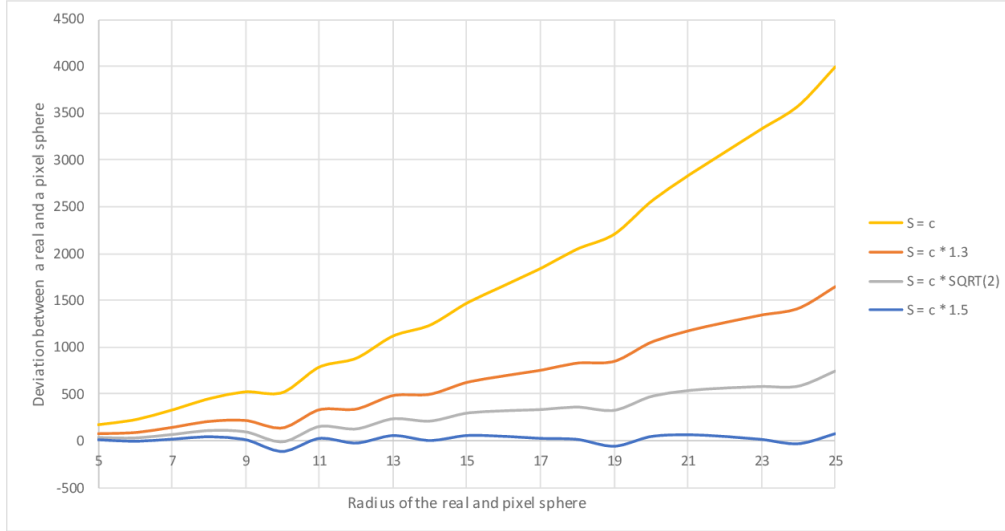


Figure 3.7: Deviation between the surface of the sphere of voxels and a real sphere. Each deviation is calculated with a different factor of the surface of the real sphere. S refers to the surface of the voxel sphere and c refers to the surface of a real sphere. Thus, $c = 4 \cdot \pi \cdot r^2$. At the x-axis the radius of the sphere and the sphere of voxels is displayed. At the y-axis the deviation between the surfaces of a sphere and a sphere cell is represented.

To receive the volume of the voxel sphere all marked entries in the created matrix are count. Then, this result is mirrored for all three axes. Thus, the amount of marked voxels in the matrix is multiplied by eight, which equals to a single multiply by two for each axis. Therefore $V = (((Voxels \cdot 2) \cdot 2) \cdot 2)$, where $Voxels$ represent the voxels in the matrix marked with a 0. To receive the surface sites of the voxels at the surface, every marked entry is checked if the voxel at $x+1$, $z+1$ or the $y+1$ is either out of bounds, i.e. if it is outside the cuboid, or outside the sphere. Every of the three conditions is checked for every voxel within the surface. If one condition is true, the amount of surface sites is increased by 1. At the end the result, like the volume, is multiplied by eight, in order to mirror the result for all three axis.

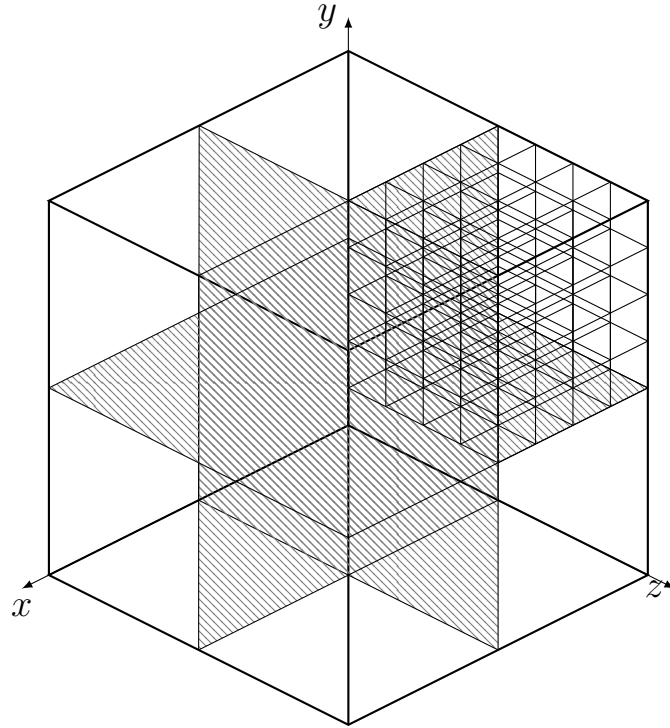


Figure 3.8: A cuboid splitted up in eight parts. This eighth of the cuboid is a cuboid itself. In order to determine which voxels are in the sphere this one eighth is filled with voxels. With these voxels it is possible to calculate the volume in voxels and the surface sites of the sphere out of voxels.

Table 3.3: An example matrix of the cuboids in picture 3.8. Each number represents one cuboid. Every column presents the voxels at a x,z coordinate whereas the entries in the row display the different voxels at the y-axis for this given x,z coordinate. 4 columns regarding to the different z-positions at one x-postion.

y3	0	0	1	1	0	1	1	1	1	1	1	1	1	1	1	1
y2	0	0	0	1	0	0	0	1	0	0	1	1	1	1	1	1
y1	0	0	0	0	0	0	0	1	0	0	0	1	0	1	1	1
y0	0	0	0	0	0	0	0	0	0	0	0	1	0	0	1	1
	z0	z1	z2	z3	z0	z1	z2	z3	z0	z1	z2	z3	z0	z1	z2	z3
	x0				x1				x2				x3			

Chapter 4

Results

This chapter presents the results of the bachelor thesis. Modifications which influence the structure of the program and the behavior of the simulation are presented at the beginning. Later the results of the desired cell as a sphere as well as the result of the created algorithm are revealed. In the last section evaluations of 3D simulations are shown.

4.1 Structure of the program

With the removal of unnecessary methods and variables, which are not used, the program becomes more readable and is easier to understand. These changes decrease the probability of errors and confusion during code analysis, i.e. studying of the code. By declaring abstract methods the program becomes more structured. Because identical methods are not written again in classes which inherit from each other it is easier to understand the program as well as to find errors.

The changes of section 3.1 and 3.2 modify the program in a way that it is more structured and understandable. This improves the time required for the code analysis, which is important for newcomers to the project, as well as to find errors.

4.2 Improvements of the program

During the bachelor thesis several adjustments in the program were made. All these changes are important for the simulation as they effect the simulation. These

changes were tested by using the output command to see the required information at the command line.

4.2.1 Calculation of the amount of stem cells on the basal membrane

With the changes of section 3.4 the program now has a calculation of the amount of stem cells on the basal membrane for two and three dimensions. The new calculation is correct for every simulation size in 2D and 3D. This is important as the program should be able to have a correct implementation for two as well as for three dimensions. An example at the initialization of a simulation is displayed in figure 4.1 at page 39.

4.2.2 MCS until the urination event

Because the calculation until the urination event was modified in section 3.3 the urination now takes place every six hours instead of every twelve hours. This change is important for the simulation because with an urination every twelve hours the simulation is not as real as with the event every six hours. Moreover, in the paper [20] of the project it is written that this event occurs every six hours. This change helps the simulation to not only be more realistic, it is also important that there are not too many cells in the simulation field. As a result of too many cells in the simulation field the simulation stops. Thus, the change increases the reality and helps to prevent an overflow of cells.

4.2.3 Target volume and target surface after mitosis

The modification of section 3.6 effects the simulation in a way that after mitosis both cells are able to grow immediately. Without the modification the cell with a too small target volume and target surface would not grow several calculation steps. Therefore, the cell does not grow several calculation steps until the target volume becomes larger than the current volume. Because the target volume of both created cells is now set dependent of the by CC3D given volume of each cell, it is not possible that one of the two cells has a smaller target volume and surface than

the current volume and surface. With this modification both cells, created during mitosis, are now able to grow immediately.

4.2.4 Conversion between the physical unit and the voxel unit

The simulation is effected in a positive way because of the changes of section 3.7. The modifications in this section are crucial since now the calculation of volume constraints of each cell type is more precise. With this modification every conversion of μm into pixels and voxels is now free of calculation errors. Because the result of the calculations of the volume constraints of the different cell types is used to determine when mitosis takes place it is important to have it without an calculation error. Because the result is converted only at the end, simulations beside a voxel density of 1 have also the correct volume constraints of the cells. Moreover, this calculation is also used to calculate the growth per calculation step in the simulation, since the growth of a cell is calculated in the physical unit and then converted into pixels. Because the calculation of the volume constraints of the different cell types and the calculation of the growth of each cell each MCS are two major parts of the simulation, this modification is important and effects the correctness of simulations.

4.3 Draw sphere cells

With the created method of section 3.8 the program is now able to draw a sphere cell, as it is displayed in figure 4.2 and 4.3 at page 42 and page 43.

Since voxels, cuboids, are used in the 3D simulation to draw a sphere cell, it is not possible to draw a perfectly round sphere. This problem is displayed with an circle and a square in picture 3.5 at page 33, since the circle and square are the 2D objects of an sphere and cuboid. The drawn cells are as spherish as possible in the simulation with the use of voxels.

Figure 4.2 displays two independently drawn cells with a radius of $5\mu\text{m}$ and $9\mu\text{m}$. These cells show that there are a lot of edges in the sphere. As the radius increases, the sphere shape of the cell gets more detailed as it is displayed in figure 4.3, in

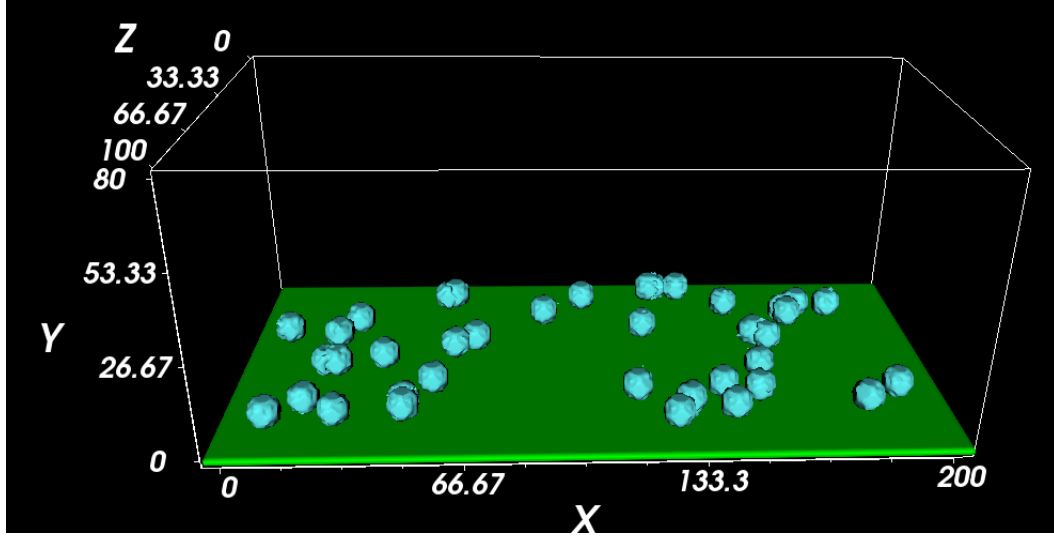


Figure 4.1: Spread stem cells at the basal membrane at MCS 0. The box displays the simulation field, with a size of $100\mu\text{m}$ at the x-axis, $80\mu\text{m}$ at the y-axis and $100\mu\text{m}$ at the z-axis. In the simulation the green bottom displays the basal membrane and at the basal membrane the stem cells are spread. The amount of these stem cells is calculated as in section 3.4 explained.

which two cells are drawn idепently with a radius of $14\mu\text{m}$ and $23\mu\text{m}$. With the increase of the radius, the deviation of the surface increases as well, as it is shown in figure 3.7 at page 34. This might be a result as the surface of a sphere and a cuboid, with the diameter $2 \cdot r$, deviates more as r increases.

4.4 Calculate the voxel volume and surface sites of a sphere cell

The created algorithm of section 3.10 is able to calculate, out of a given radius, the volume of a sphere cell created with cuboids in voxel, as well as it is able to count the surface sites of the cell. Moreover, it is also possible to calculate the physical volume and surface of a sphere with a given radius. With this algorithm it is possible to calculate the volume and surface of a sphere cell and get the same result as CC3D calculates.

The algorithm is useful but also has its weaknesses. For a voxel density beside 1 the results between the created algorithm and CC3D deviate. The results differ also if the radius is not a whole number. There are no insights how CC3D calculates the volume and surface of a drawn sphere cell. Moreover, for the tenths part of five to nine of the radius, for every radius between .5 until .9, it is possible to create the cube with an radius which is either rounded up or down. This means for a radius of

3.7 it is possible to use either six or eight voxels to create the cuboid. Seven voxels are not possible because then the sphere would lose its symmetry.

The algorithm helps to calculate the volume of a sphere cell, out of voxels, as well as to count the surface sites. It is able to be executed without a start of a simulation. Thus, there is no need to adjust the coding of the project and to wait until the simulation started to receive the volume and surface values of a sphere cell.

4.5 Grow sphere cells

In section 3.9 the factor for the calculation of the surface of the cell was evidenced best to be 1.5 for a voxel density of 1. With this factor it should be possible to let the sphere cell grow as a sphere. To test the growth of the cell, one single cell was placed in the simulation field. As the cell grew during the simulation the volume and surface values were read out of the command line and compared to the documented values of a drawn cell.

To let a cell grow as a sphere does not work. Even the volume and surface values, calculated by CC3D, and the target volume and target surface values, calculated by the program, meet the values of sphere cells with a small deviation of a maximum deviation up to 50 voxels.

In figure 4.4 and 4.5 at page 44 and 45 examples of the growth of two stem cells with a different radius are displayed. It is observable that these cells are not able to keep the shape with which they were depicted.

4.6 Adhesion

The new adhesion matrix is different than the one which was used until this thesis. Out of the observations of section 3.5 the new adhesion matrix was created. The matrix is displayed in table 4.1. The values were chosen in a way that cells of one layer stick to each other and try to increase the area where the cells touch. The adhesion for cells at one layer was observed not to be too high in order that the cells do not infiltrate each other. An example therefore is displayed in figure 4.6 at page 46. If cells infiltrate each other it is a sign of too high adhesion energy. For the adhesion between cells of different layers in the urothelium the values were chosen in a way that the cells connect with each other but that they grow independently. It

is important that the cells of different layers do not connect too strongly to each other, otherwise the different layers in the urothelium might be mixed.

Table 4.1: New adhesion values for the adhesion between the different cell types. M, the medium cell type, is a by CC3D specific cell type for the simulation.

Types		M	BM	S	B	I	U
Medium	M	0	14	14	14	14	14
Basal membrane	BM		-1	2	3	30	30
Stem cell	S			12	15	25	25
Basal cell	B				12	25	25
Intermediate cell	I					6	25
Umbrella cell	U						2

4.7 Simulations

To test this bachelor thesis some 3D simulations were made. It would be nice to have an in depth analysis of several simulations. This is not possible because a 3D simulation over a timespan of 700 days with a simulation field of $200\mu\text{m}$ at the x-axis, $80\mu\text{m}$ at the y-axis and $100\mu\text{m}$ at the z-axis and with a voxel density of 1 took 14 days to complete. Because this immense time effort a brief analysis of one simulation run of the model SPA/PCDB/PCDI is provided. In the next chapter analyses of short simulations are compared briefly to the completed simulation presented in this chapter.

Figure 4.8 at page 47 displays screenshots at the front and at the back of the simulation field. These screenshots are taken after simulation was finished. It is visible that the arrangement of the cell layers is not perfect, because some umbrella cells are at top of the basal cells. Moreover, at one point an intermediate cell is surrounded with umbrella cells, therefore it is at a wrong layer in the urothelium.

In figure 4.7 at page 46 a result of the fitness functions of sections 2.8.1 and 2.8.2 is provided. The arrangement fitness function displays an almost perfect result of an urothelium, whereas the volume fitness function displays not much reality in the simulation. The analysis of this simulation and of other simulations is discussed in the next chapter in section 5.6.

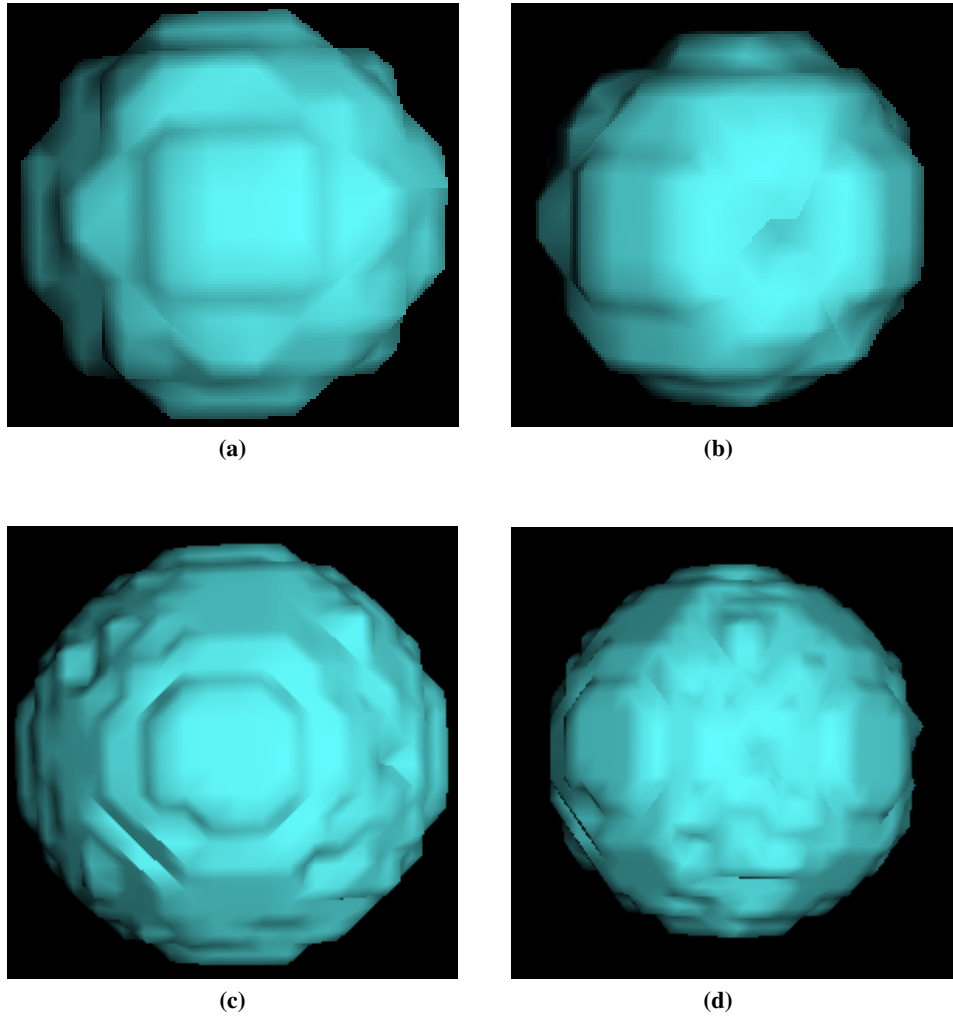


Figure 4.2: A single cell drawn into the simulation field. The radius of the cell of (a) and (b) is 5 and the radius of the cell of (c) and (d) is 9. Pictures (a) and (c) are with the front view, whereas the pictures (b) and (d) have a view angle of around 45 degrees. The color of the cell is chosen in a way that more details are visible.

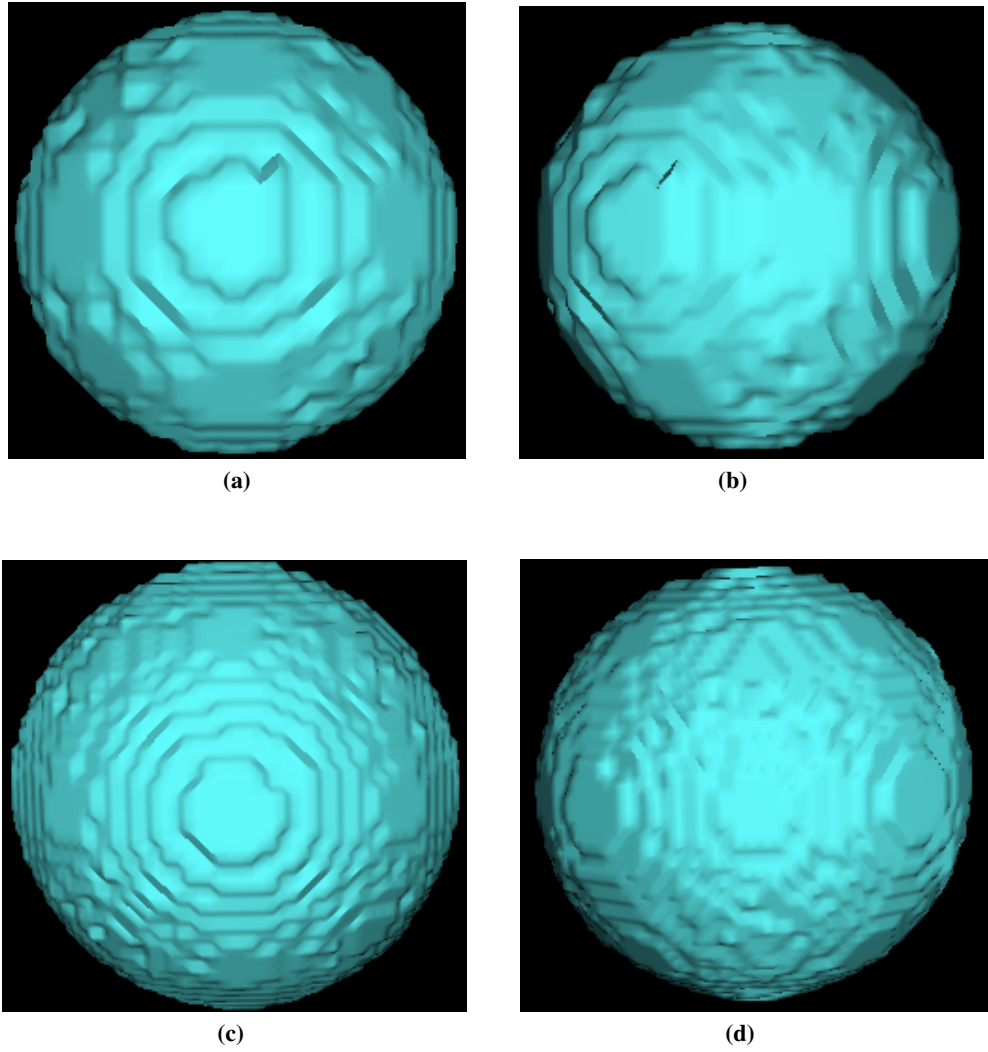


Figure 4.3: A single cell drawn into the simulation field. The radius of the cell of (a) and (b) is 14 and the radius of the cell of (c) and (d) is 23. Pictures (a) and (c) are with the front view, whereas the pictures (b) and (d) have a view angle of around 45 degrees. The color of the cell is chosen in a way that more details are visible.

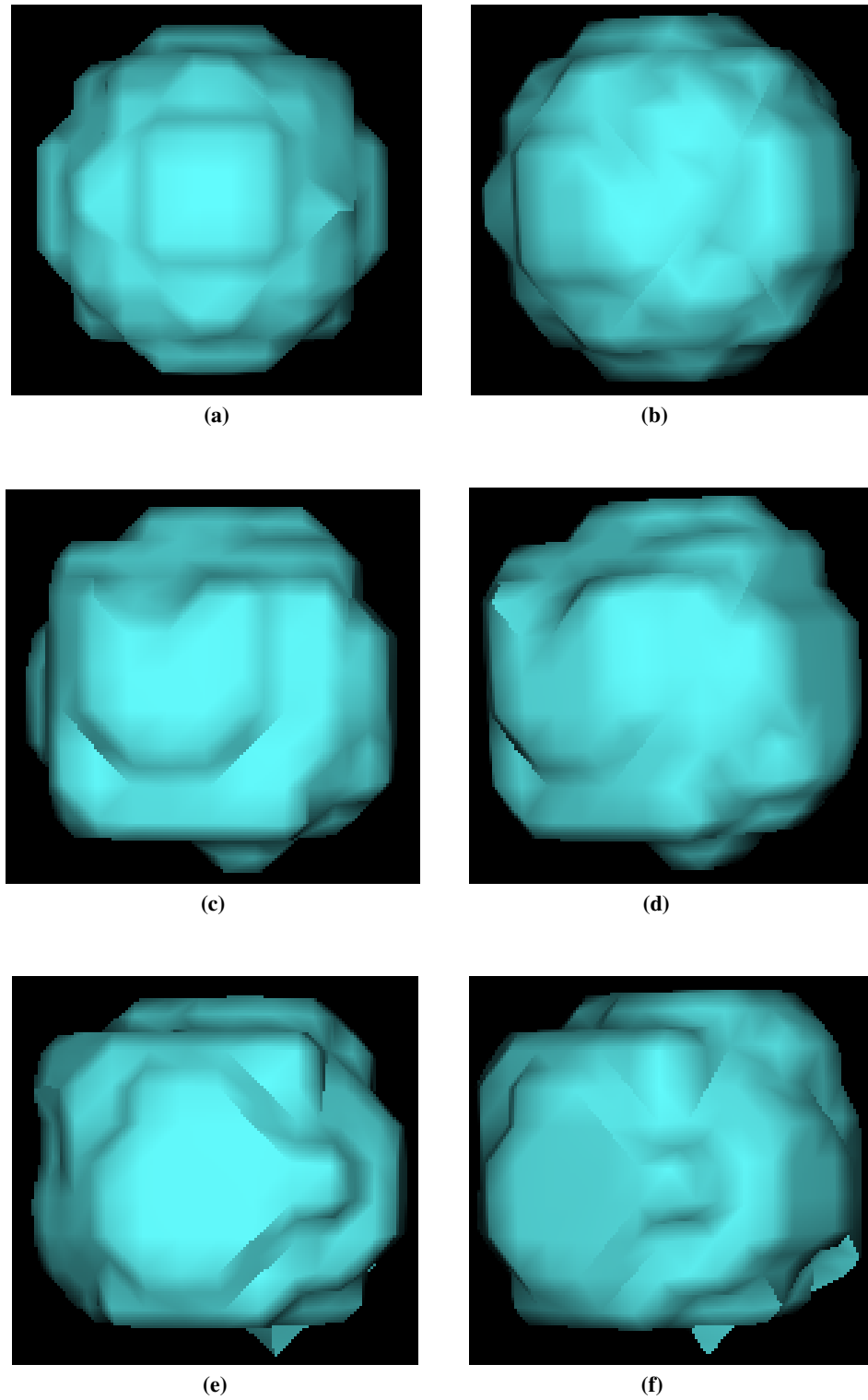


Figure 4.4: A sphere cell, with a radius of $5\text{ }\mu\text{m}$ and a voxel density of 1, as it grows. Images (a), (c) and (e) are the front view of the cell and figures (b), (d) and (f) have around a 45 degrees angle of the front. Figure (a) and (b) are at MCS 0, images (c) and (d) at calculation step 50 and figures (e) and (f) present MCS 250.

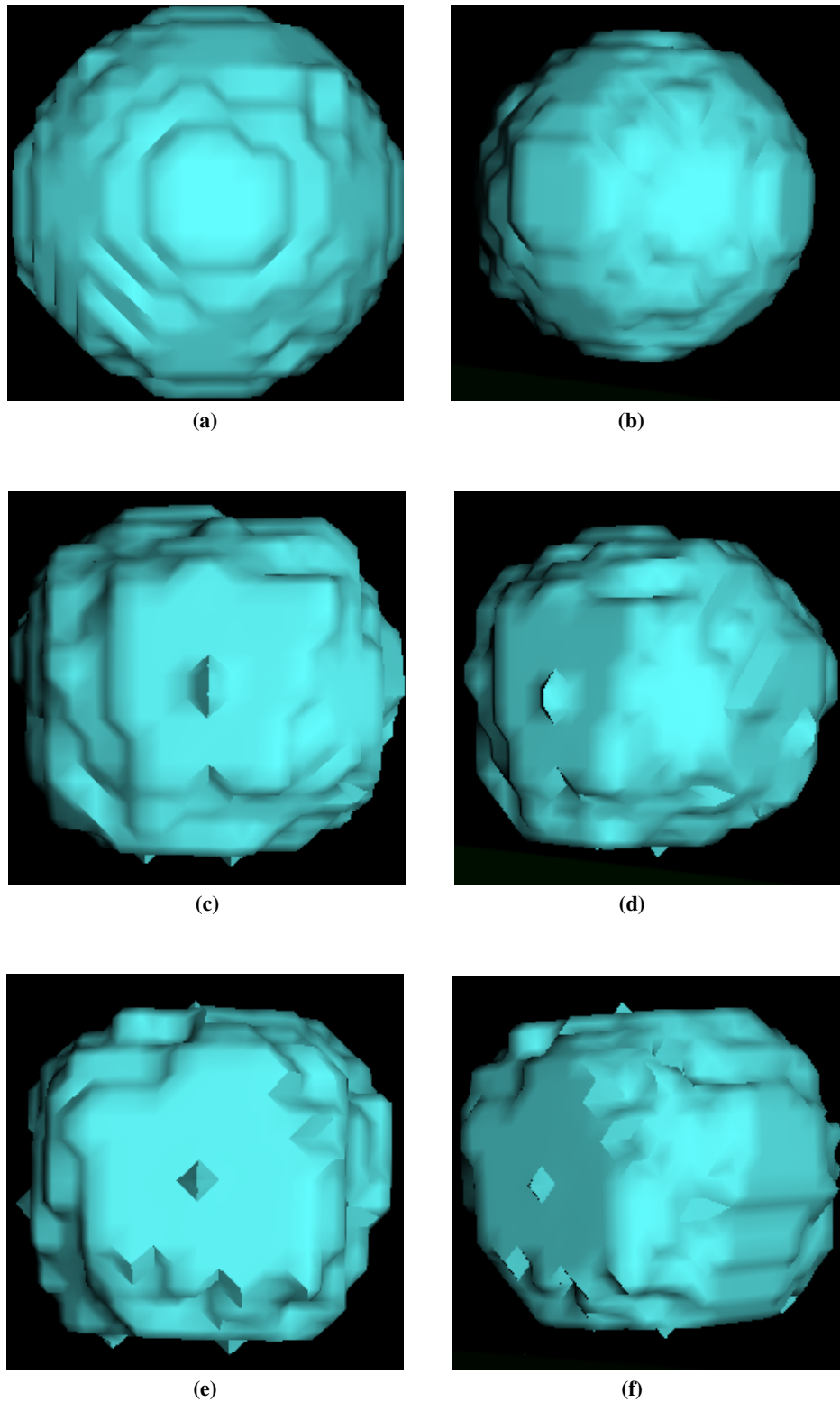


Figure 4.5: A sphere cell, with a radius of $9\mu\text{m}$ and a voxel density of 1, as it grows. Images (a), (c) and (e) are the front view of the cell and figures (b), (d) and (f) have an approximately 45 degrees angle of the front. Figures (a) and (b) are at MCS 0, figures (c) and (d) at calculation step 250 and figures (e) and (f) present MCS 750.

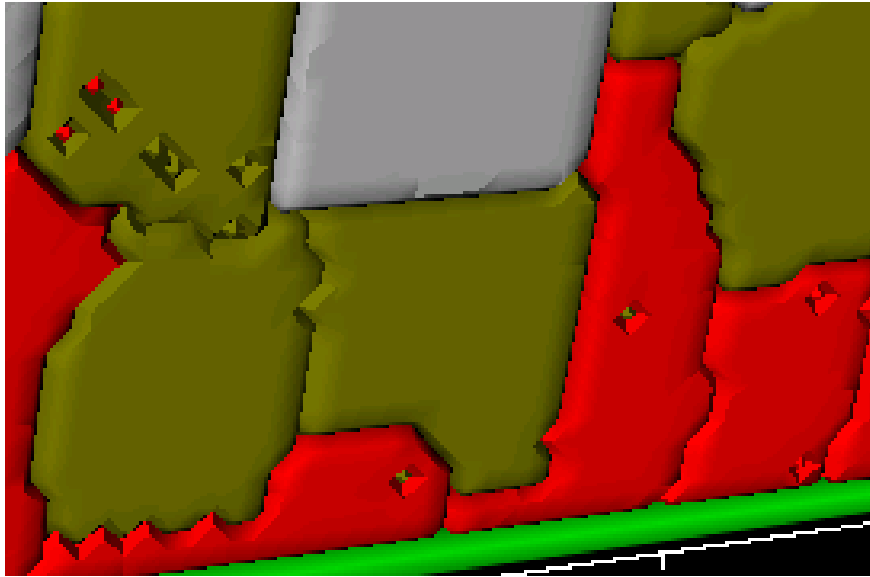


Figure 4.6: Different cells try to infiltrate each other as a reason of too high adhesion values between the cells. The different points at the surface of a cell are an indicator that a surrounding cell tries to infiltrate the cell at which the points occur.

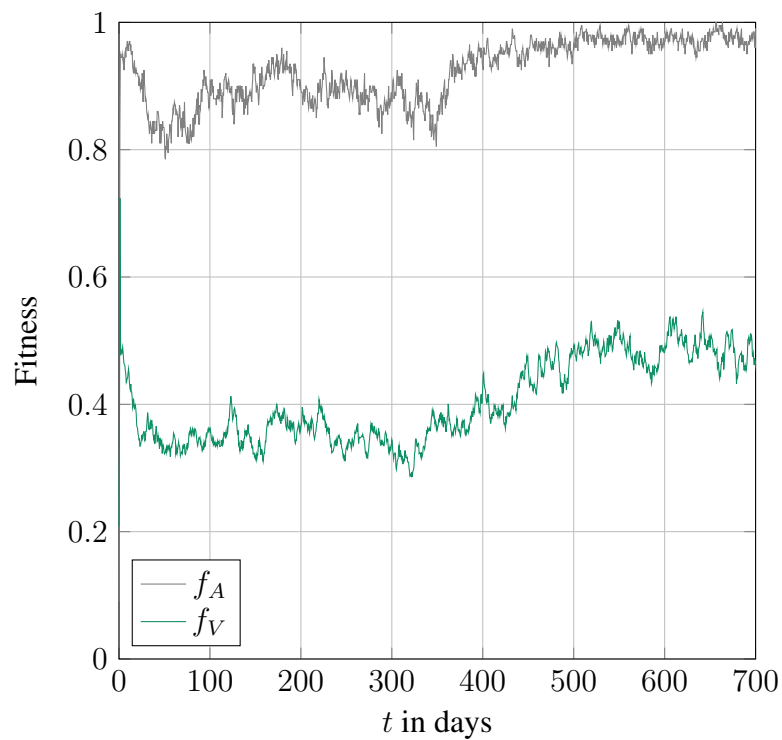
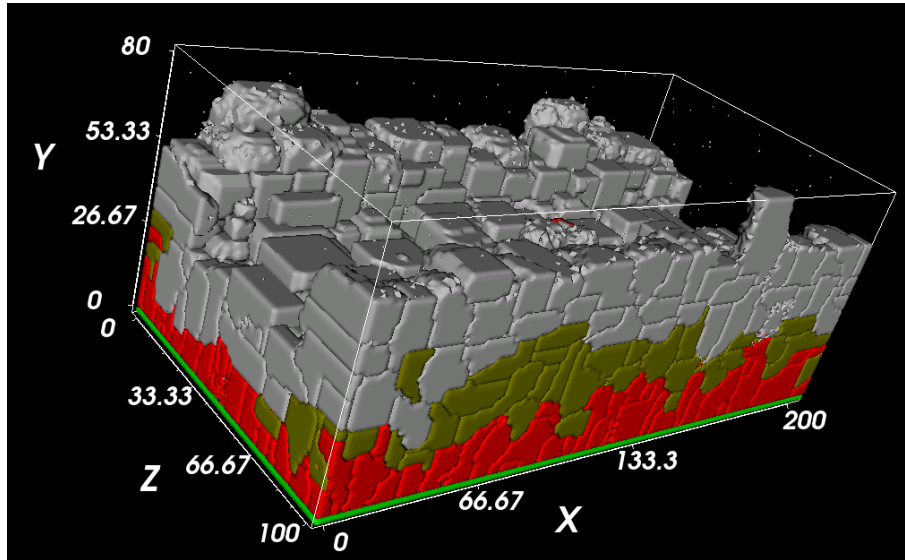
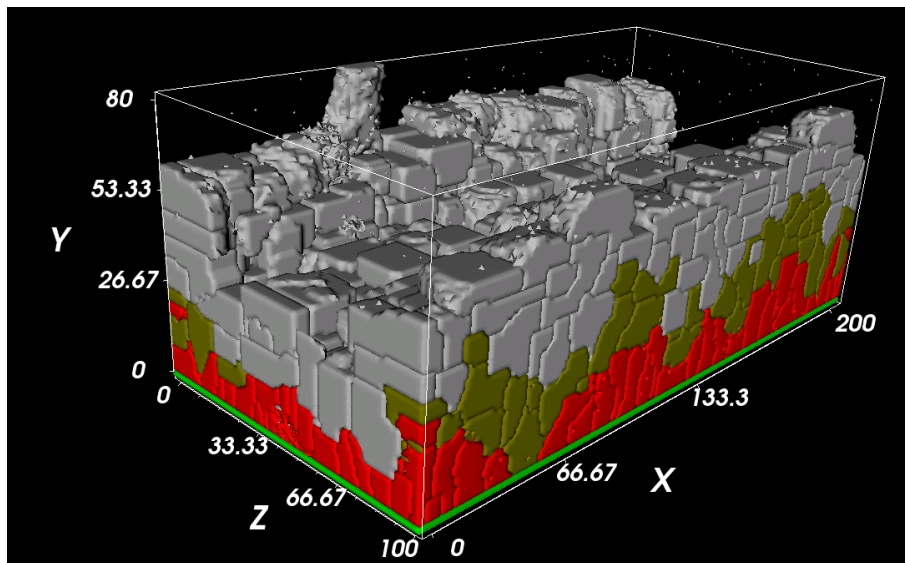


Figure 4.7: An analysis of an simulation of the model SPA/BCPD/IPCD. The simulation covered 700 days, 350000 MCS. The analysis covers the arrangement, f_A and the volume fitness function, f_V of sections 2.8.1 and 2.8.2. At the figure the 'Fitness' values represent the reality of this model, where 0 refers to no reality and 1 presents a perfect realistic simulated urothelium.



(a)



(b)

Figure 4.8: Screenshots at the end of a simulation of the model SPA/PCDB/PCDI, which lasted 700 days. Screenshot (a) is taken of a front view, whereas screenshot (b) is taken of the back of the urothelium.

Chapter 5

Discussion

In this chapter the developed solutions and the results are discussed from different aspects. Problems, which occurred during the bachelor thesis, are presented as well.

5.1 Cell as a sphere

To draw a sphere cell is one way to get the desired spherish shape of the cell. Sadly, to keep the shape of the cell during the growth process does not work. Because for a given volume and a given surface there are all kinds of possible shapes, CC3D does not know which shape the cell should have. It is suprising that every time during the growth process the cells get a shape similiar to a cube. It might be a result of the square lattice, which is used in the simulation. Another interesting fact is that smaller sphere cells get a form of a cube faster during the growth process than sphere cells with a larger radius. This might be a result of the larger radius. Figure 4.4 and 4.5 at page 44 and 45 display such a fact. It is observable that the cell with a radius of 5, at illustration 4.4, has a form of a cube after 50 MCS whereas the larger sphere cell gets a form like a cube after 250 MCS. A sphere cell with a smaller radius has less details and therefore it is more likely that this one is formed into a cube than a sphere cell with a larger radius.

There are several research papers, which use CC3D for their simulation, sadly it is never explained how the desired cell form is achieved neither which lattice type is used. Some of the literature is linked at the homepage of CC3D [12]. So far, it is not possible to know if there is a mistake in the simulation or if the cells get shape similiar to a cube due to the square lattice.

Because CC3D only determines the shape of the cells, there are other techniques to reach the shape of a sphere cell. It is possible that a cell reaches a desired volume and surface, by only setting the terms for the volume and surface of the effective energy. The desired values can be reached faster if a high multiplier, λ_{vol} and λ_{sur} , is set. This has the disadvantage that a volume or a surface constraint might weigh more than the term of the adhesion in the effective energy. If the specific multiplier has a small value, it might be possible that it takes a long time until the desired shape is reached. In addition to the volume and surface constraint comes the adhesion. The new adhesion matrix is discussed in the next section.

5.2 Adhesion

Adhesion influences the shape of two or more cells, as it describes how strong the cells stick to each other. If the adhesion is set too high the cells infiltrate each other but if it is too low the cells may not stick to each other as they change their shape. An example therefore is displayed at figure 4.6 at page 46. During the simulations with the old adhesion matrix it was observable that some cells of different cell types want to infiltrate each other. This is a result of too high adhesion. With the new adhesion matrix it still appeared that sometimes cells want to infiltrate each other. In the new adhesion matrix, displayed in table 4.1 at page 41, the adhesion energy between the cells is already loosened up. Because the adhesion was observed with two cells in a simulation field, this observation might be not precise enough to be used in the simulation. This would be a reason that in a simulation the cell is surrounded by other cells and therefore the results of the observation might not completely apply during a simulation. To find the perfect suiting adhesion values observations during simulations should be made. The problem is that this technique is too time consuming although it would be useful. Maybe it is already enough to reduce the adhesion between the cell types, in which the cells wanted to infiltrate each other, but maybe it is also required that additional observations of the different adhesion values have to be made.

5.3 Voxel Density

In the simulations the voxel density should be set to 1. In this case, in CC3D one $1\text{ }\mu\text{m}$ is presented by one voxel. If the voxel density is higher than one voxel represents less μm . Because the simulations requires a lot of more time if the voxel density is high and the deviation between the volume and surface values of a sphere cell and a real sphere are larger, it should be tried to keep the voxel density as small as possible but also not to small. If the voxel density is too small than less details can be displayed and it is much more likely that the cells do not look like spheres. Why the deviation of the volume of a cell and a real sphere grows so much more for a higher voxel density, as it is displayed in figure 5.1, is a puzzle.

On one hand the deviation of the volume and the surface grows with the radius, with more voxels. Since with a higher voxel density there are also more voxels to display it might be a result that CC3D uses more voxels to display the cell. On the other hand, with a voxel density of 2, the volume and surface values of the drawn cell are that high that for the surface of a real sphere a factor of six would give an approximation to the surface of the drawn cell.

The surface of the cell is one factor, but as it is displayed in table 2.3 at page 19 the correct volume is more important than the surface. In figure 5.1 the volume of a real sphere and of a drawn sphere cell in CC3D are too far apart as this voxel density is useful for a simulation. It is interesting to observe that the volume of a sphere cell increases this fast, whereas the surface of a sphere grows in an almost linear way for an increasing radius. Since in CC3D in a 3D simulation the volume refers to a physical volume and the surface refers to a physical surface it might be that one voxel still represent $1\text{ }\mu\text{m}$, even it should be only $0.5\text{ }\mu\text{m}$. This might explain the results, as they are similiar to the results of $2 \cdot r$ if the voxel densitiy is 1.

As a voxel density of 2 is not useful for the simulation, the same case happens with a voxel density of 0.8. As it is displayed in figure 5.2 at page 52 the surface of a real sphere and a sphere cell do match but the volume of the sphere cell does not grow fast enough. Because the volume of the sphere cell does not grow fast enough it deviates more with a growing radius to the volume of a real sphere.

Image 5.3 at page 53 displays how well the volume of a sphere and a sphere cell in μm fit for a voxel density of 1. For this voxel density the volume of the sphere and the sphere cell are so close to each other that there is no visible deviation in the image. In this image a further reaching radius was chosen to demonstrate this fact.

Because there is almost no difference between the volume of a sphere and a sphere cell the voxel density of 1 should be used in the simulation. Another advantage of this voxel density is that no conversion errors between the voxel unit and the physical unit in μm can occur.

Why the volume and surface values of a sphere and a sphere cell deviate for the different voxel densities is a mystery. The values of a sphere cell for all three voxel densities are taken only of the by CC3D drawn cell. Because the values are calculated by CC3D it is possible that it is their mistake but it is also possible that the different deviations are normal and they were not discovered or explained in the literature yet.

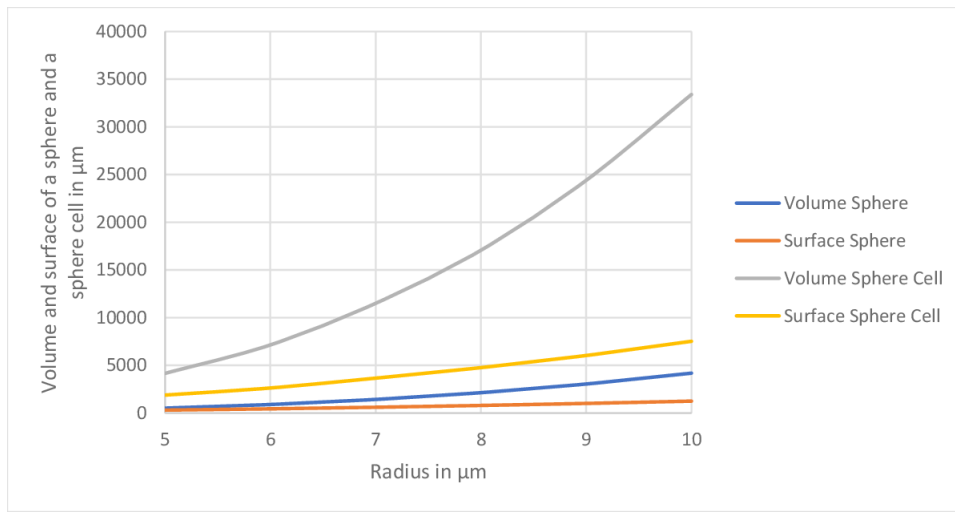


Figure 5.1: Volume and surface in μm between a sphere and a sphere cell for a voxel density of 2. The lines 'Volume Sphere' and 'Surface Sphere' display the volume and the surface of a sphere. The lines 'Volume Sphere Cell' and 'Surface Sphere Cell' display the volume and the surface of a sphere cell.

5.4 Surface approximation

The approximation of the surface of a cell to a surface of a real sphere is done with voxels, because these are also used in the simulation field. There are other techniques to approximate the surface of a sphere. It is possible to use pyramids for this approximation. Since in the current simulation the square lattice is used it might be difficult to find an approximation technique which suits the square lattice better. Moreover, the volumes of the cells and of a sphere are almost identical for the same radius, if the voxel density is 1. Because the volume of a cell is more important than

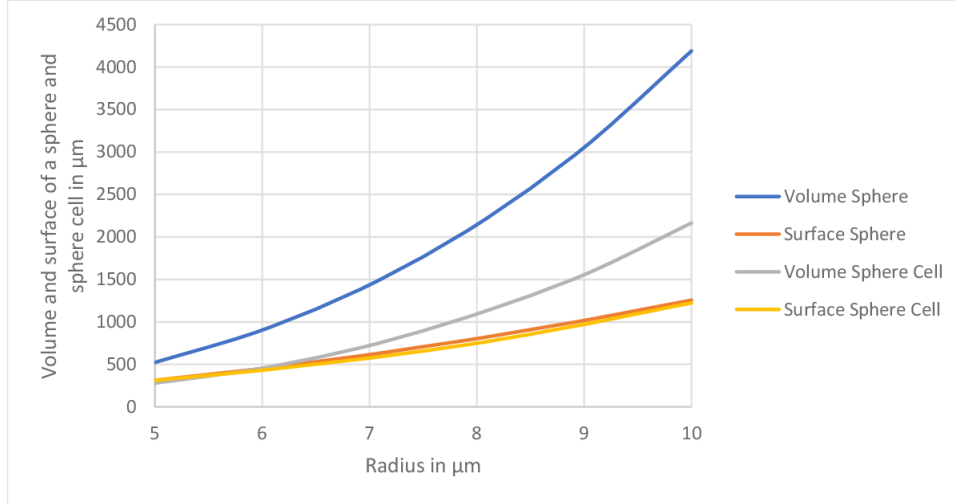


Figure 5.2: Volume and surface in μm between a sphere and a sphere cell for a voxel density of 0.8. The lines 'Volume Sphere' and 'Surface Sphere' display the volume and the surface of a sphere. The lines 'Volume Sphere Cell' and 'Surface Sphere Cell' display the volume and the surface of a sphere cell.

the correct surface, as it is listed in table 2.3 at page 19, a new approximation has to be checked against its volume as well as its surface. The use of pyramids might be in general a great way to approximate a sphere but for the square lattice it might be not as suited as it uses cuboids.

5.5 Surface Variation Pixels to Sphere

The created algorithm of section 3.10 has its benefits and also its weaknesses. There are several ways to design the algorithm. One is to use the same method as it is used to draw the sphere cell. With this method every voxel in the cuboid has to be checked if it is inside or outside the algorithm. Therefore, a lot of calculations are required to create the matrix of the cuboid, with the radius two times larger than the one of the sphere, from which the volume and surface sites can be calculated. This amount of calculations is r^3 , where the radius of the cuboid is $2 \cdot r$, as it is explained in section 3.8. Thus, the amount of calculations to create the algorithm is $(2 \cdot r)^3$, where r is the radius of the sphere. Because this approach has a high computational cost it should be only used if it is necessary.

The next two approaches are similar. Both split the cuboid and the circle up into eight pieces, then the calculations are done with one of the eight cuboids and as last step this result gets mirrored. This is possible because a cuboid split up into

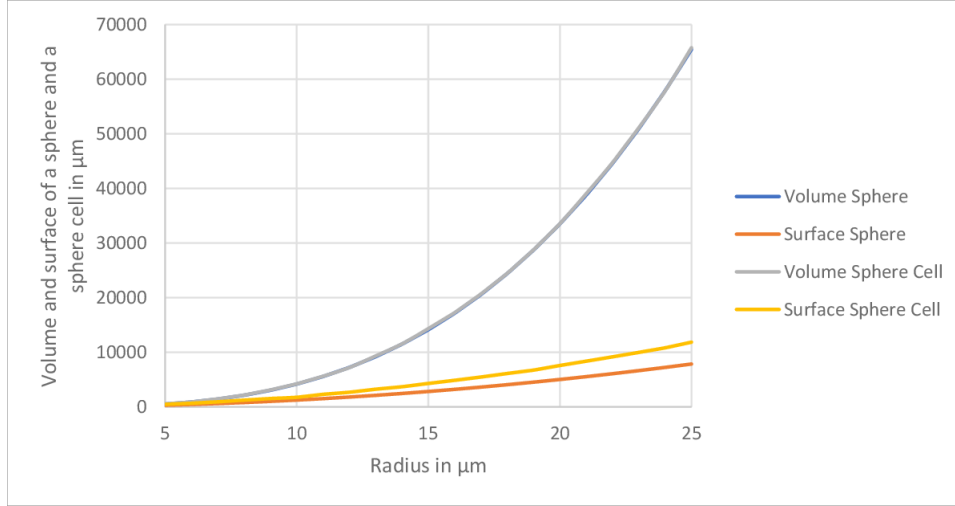


Figure 5.3: Volume and surface in μm between a sphere and a sphere cell for a voxel density of 1. The lines 'Volume Sphere' and 'Surface Sphere' display the volume and the surface of a sphere. The lines 'Volume Sphere Cell' and 'Surface Sphere Cell' display the volume and the surface of a sphere cell. The line 'Volume Sphere' is not visible because it lays under the line 'Volume Sphere Cell'. The deviation between these values is so small that only one line is displayed.

an odd amount of parts creates several smaller cuboids. With this small cuboid it is possible to calculate if every cuboid, in the small cuboid, is inside the sphere. Then the matrix is created. For the calculation of the volume and surface the result of the one eighth of the cuboid is mirrored for all three axes. This approach has less computations than the approach before. The amount of computations is now $(\frac{r}{2})^3$. Because only the half of the radius of the sphere is used, this is an improvement over the approach before.

The approach with the least computational cost is similar to the one before. After the cuboid around the sphere is split up into eight pices, the point in which the circle is at a given x,z coordinate is calculated. Then it is checked which cuboids at this given x,z coordinate are within the circle or not. Based on this approach there are even less calculations. Because of the eighth of the cuboid only the height of the circle for a given x,z coordinate is calculated. The required amount of calculations is now $(\frac{r}{2})^2$. Because one eighth of the cuboid is used, the half of the radius of the sphere is required. Moreover, only every x,z coordinate is needed for the calculations, instead of every x,y,z coordinate of the cuboids. Thus, the approach of the algorithm has the lowest computational cost. Even the algorithm has its weakness, it has a good basis to be further developed.

5.6 Simulation Results

During this bachelor thesis one simulation has been finished. This simulation took 14 days to complete, therefore no other simulation had a complete simulation run. Other simulations were simulated 20 up to 50 days. First the completed simulation will be discussed and then aspects of the other simulations are included.

It is interesting to see that both fitness functions have an increase after almost one year, as it is displayed in figure 4.7 at page 46. Why this increase happens for both fitness functions at the same point is a puzzle. The problem is that only the cells at the edges and sites are visible but there is no quick overview of the inside of the simulated urothelium. Another interesting fact is that the simulated urothelium has in the middle less cells than at the edges. This might be a result of the urination event, as the cells which are removed are randomly chosen. It would be interesting to see if this happens for other simulations as well or if it happens by incident.

A similarity of all simulations is that the result of the arrangement fitness function always decreases in the first 50 days. Because in the finished simulation this is also the case and it increases later in the simulation. No statement can be done if this decrease of the arrangement fitness function is normal or not. For the result of the volume fitness function no similarities of the different simulation runs were found. Maybe there would be some similarities visible for a longer duration of the simulations.

5.7 CC3D

Several simulation programs have been tested in an earlier master thesis of the project [21], it was evidenced that CC3D is the best suited program. During this bachelor thesis several weaknesses of CC3D were realized. Those are explained in the following paragraph.

To develop a program a debugger should be available. A debugger allows the developer to execute the program command wise and to observe the values of the variables in the program. CC3D does not offer a debugger. Therefore every observation of a variable or the order of the function calls has to be printed to the command line. This has significant disadvantages, as it requires more time to understand the structure of the code as well as the print commands first have to be written. Moreover, the developer has to be very precise at the print commands and

she / he needs to know which output at the command line belongs to which print command.

A second disadvantage is that the memory after a simulation is not released. Every simulation requires a specific amount of memory dependent of the simulation field size. This memory should be released after the simulation is finished. If the memory would be released after the simulation other programs could use it. Moreover, by starting a simulation after another simulation is finished, CC3D reserves the memory for the new simulation in addition to the required simulation before. Therefore, by starting several simulations without closing CC3D, the program has a high probability to crash because there is not enough memory free for the simulation.

Because the required memory for a simulation increases as the size of the simulation field increases it is good to know where the constraints of the size of the simulation field are. The size constraints were tested on a Virtual Machine (VM) with the distribution 'Windows 7' as a 64 bit version. The VM has a memory of 4GB. For this memory the constraint of the size of the simulation field is around by 400 voxels for each axis. Therefore, around 107171875 voxels are allowed in the simulation. For this size of the simulation field CC3D became very slow, which is a result of the amount of memory. This constraint is different for different distributions as well as for different sizes of the memory.

5.8 GGH Model

The GGH model is widely used because it is easy to use. Even it is easy to use some parameters of the approach are not explained in detailed. As example it is possible to set a temperature for the simulation. This temperature effects how much a cell fluctuates as it changes its volume or surface. That the fluctuations changes with a different temperature is observable. Because it is almost nowhere explained it is questionable if this is the only effect of the temperature in the simulation or if there are other effects with it.

For the scenario with the sphere cell it is a disadvantage that it is not possible to set a constraint of the shape of a cell. The use of one radius or one diameter would already be enough to limit the amount of possible shapes of a cell for a given volume and surface. Because such a constraint can not be set and it is not explained in the literature how to receive a specific shape of a cell a lot of experiments have to be done to reach the desired shape of the cell.

Chapter 6

Future work

This chapter provides suggestions as well as ideas for the project. These suggestions and ideas could have a positive impact on the project. At the beginning suggestions for the project are made. Then, ideas for the future of the project are mentioned.

This first point is not really an idea it is more a strong suggestion. It has to be decided if the fitness functions out of the 'OptimumSearchSteppable' or out of the 'VolumeFitnessSteppable', 'ArrangementFitnessSteppable' and 'DummyFitnessSteppable' are used in the project. In the paper of the project [20] the formulas of both techniques are mixed and in the program the functionalities of the three steppables are used. The techniques differ in the formulas for the volume and arrangement fitness function. Only the technique out of the 'OptimumSearchSteppable' includes the total fitness function. It is surprising why both techniques are included in the project even if only one technique is used.

Both techniques have to be evaluated and then it has to be decided which one should be used. Because these techniques cover the fitness functions and therefore the analysis of an simulation, it is crucial for the correctness of the analysis of the simulations as well as for the future of the project to decide between one of the functionalities.

Because the improvements of sections 3.3, 3.6 and 3.7 and the findings of section 5.3 the 2D simulations should be checked again. The changes of the named sections affect the simulation no matter if it is done in two or in three dimensions. Therefore, a check if the results of the 2D simulations are still the same might be appropriate. Additionally it should be verified if these results are the same for a voxel density of 1. If the results differ from the findings so far it might be important to redo the 2D simulations with a voxel density of 1 before continuing with the 3D technology.

As the result in section 4.5 reveals to keep a sphere shape is not possible. Because it might be a result of the square lattice it should be tested if the hexagonal lattice type suits this task better. With the hexagonal lattice the cells are hexagons in 2D and rhombic dodecahedrons in 3D. Because a rhombic dodecahedron is in its form already similar to a sphere it might work to keep the sphere shape of a cell with these objects.

In addition to the different lattice type it should be tested if another approximation to the surface and volume of a sphere is possible. A possible approximation is to use pyramids. With the use of the hexagonal lattice type the cells are made of rhombic dodecahedrons, in three dimensions. The rhombic dodecahedron consists of twelve polygons, where each of the twelve polygons is a pyramid itself. In case of a dodecahedron all parts have the same area as well as the same shape [22]. An explanation of the rhombic dodecahedron and some basic calculations can be found at Wolfram MathWorld [23].

As an extension of the project malignant cells could be simulated. Because these cells behave different from the non-malignant cells it will be a challenge to implement these cells. This could increase the reality of the simulation a lot. First the hexagonal lattice should be tried to get sphere cells and a solid 3D simulation. It might be a useful extension if the 3D simulation works properly.

CC3D showed some weaknesses during the bachelor thesis. It is used for several years in the project and therefore there is a good knowledge how to handle the weaknesses. Beside the weaknesses CC3D has also its strengths. It allows to develop a simulation program in several programming languages. This brings freedom to the developers as they can choose if a more object oriented or a script oriented program is used. It would be very useful, especially for complex programs, if a debug during the simulation would be possible. Another strength of CC3D is that it has a very active community. In the community a lot of questions are asked and members of the project as well as other community members help as much as possible. Therefore, it is possible to ask the community and get a feedback regarding the problem soon. CC3D is not the only program which could be used. In a masters thesis of a former student it was evidenced that it is the best suited program for the simulation of the urothelium [21] at this time. This evaluation is almost four years in the past. Therefore, it might be possible that there are other programs as well as other approaches which could be used. One possible program would be Morpheus. It is developed at the technical University in Dresden. In the most recent paper, in which the program

is used, a 3D multi-scale model of fluids in the liver was simulated [24]. Another program for the simulation might be Biocellion. It uses a parallel developing approach. This means the hardware sources of the computer can be used more as it is possible to let the cores of a CPU do several tasks [25]. It might be suited for this problem because a cell has a sphere shape by default [25]. These two programs could be an alternative to CC3D.

An approach which uses parallelization is the Random Walker (RW) algorithm [26]. This approach uses the CPM algorithm. With the created RW algorithm a speedup of 3 to 10 times in comparison to the CPM is possible [26]. It is also mentioned that it is not enough to have a fast algorithm which allows parallelization, the developer has also to know how to use the algorithm in order to develop a faster simulation. These programs and approaches might be an alternative to CC3D. To determine if CC3D is the best suited program for the morphogenesis simulation of the urothelium, it might be useful to do a new evaluation of the different algorithms and programs for cell simulation at the market.

Chapter 7

Conclusion

After this journey the 3D simulation of the urothelium is possible. During this bachelor thesis several important changes at the program and crucial observations were made.

With the modifications of this thesis it might be useful to evaluate the results of the 2D simulation again before the 3D simulation is done in the next step. Then, it is possible to further search for techniques to get a sphere cell within the 3D simulation.

In the end, it is now possible to use the 3D simulation. Together with members at the Clinic of Urology the evaluations of the 2D simulations as well as the results of the 3D simulations should be analyzed. These evaluations of the 2D and 3D simulations can be used to find new patterns and insights on the question how bladder cancer arises.

List of Abbreviations

GGH Glazier-Graner-Hogeweg

CC3D CompuCell3D

MCS Monte Carlo Step

CPM Cellular Potts Model

EPM Extended Potts Model

OOP Object Oriented Programming

RW Random Walker

VM Virtual Machine

List of Tables

2.1	16 different models in the project	18
2.2	Adhesion matrix, which was used earlier in the project	19
2.3	Constraints of the different cell types	19
3.1	Approximation errors of a not rounded result, with which it is further calculated	24
3.2	Different calculations of the conversion of a physical unit into the voxel unit	27
3.3	A matrix to determine which voxel is within the sphere or not	35
4.1	New adhesion values for the different cell types	41

List of Figures

1.1	A simplified illustration of the urothelium	4
1.2	A two dimensional square lattice	5
2.1	Initial state of a 2D simulation of the model SPA/BPCD/IPCD . . .	10
2.2	2D Simulation of the model SPA/BPCD/IPCD after 33 days	11
3.1	Considered area to spread the stem cells in two dimensions	23
3.2	Considered area to spread the stem cells in three dimensions	23
3.3	A cuboid layed around a sphere	28
3.4	A cuboid with minimal size layed around a sphere in two dimensions	30
3.5	A circle in a possible pixel presentation	33
3.6	An approximation to the surface of a sphere with a pixel and a diagonal	33
3.7	Deviation between the surface of the sphere of voxels and a real sphere	34
3.8	A cuboid split up into eight parts. One eighth is filled with voxels. .	35
4.1	Spread stem cells at the basal membrane at MCS 0	39
4.2	Drawn sphere cells with a radius of 5 and 9	42
4.3	Drawn sphere cells with a radius of 14 and 23	43
4.4	Growth of a sphere cell with a radius of 5	44
4.5	Growth of a sphere cell with a radius of 9	45
4.6	Different cells try to infiltrate each other	46
4.7	Analysis of a simulation of the model SPA/BCPD/IPCD	46
4.8	Simulated urothel with the model SPA/PCDB/PCDI at day 700 . . .	47
5.1	Volume and surface in μm between a sphere and a sphere cell for a voxel density of 2	51
5.2	Volume and surface in μm between a sphere and a sphere cell for a voxel density of 0.8	52
5.3	Volume and surface in μm between a sphere and a sphere cell for a voxel density of 1	53

Listings

3.1	Initialization of an class variable in order to use the library ABC . .	21
3.2	Declaration of an abstract method	21
3.3	Modified function to calculate the volume of a cell in voxel out of a physical volume	26
3.4	Created function to draw a sphere cell	30

Bibliography

- [1] N. J. Poplawski, U. Agero, J. S. Gens, M. Swat, J. A. Glazier, and A. R. A. Anderson, “Front instabilities and invasiveness of simulated avascular tumors”, *Bulletin of Mathematical Biology*, vol. 71, no. 5, pp. 1189–1227, Jul. 2009. DOI: 10.1007/s11538-009-9399-5. [Online]. Available: <https://doi.org/10.1007/s11538-009-9399-5>.
- [2] [Online]. Available: <https://www.everydayhealth.com/bladder-cancer/guide/>.
- [3] [Online]. Available: <https://www.cancer.org/cancer/bladder-cancer/about/what-is-bladder-cancer.html>.
- [4] M. Lazzeri, “The physiological function of the urothelium—more than a simple barrier”, *Urologia internationalis*, vol. 76, no. 4, pp. 289–295, 2006. DOI: <https://doi.org/10.1159/000092049>.
- [5] T. Yamany, J. Van Batavia, and C. Mendelsohn, “Formation and regeneration of the urothelium”, *Curr Opin Organ Transplant*, vol. 19, no. 3, pp. 323–330, Jun. 2014. DOI: 10.1097/MOT.0000000000000084.
- [6] L. A. Birder, “More than just a barrier: Urothelium as a drug target for urinary bladder pain”, *American Journal of Physiology-Renal Physiology*, vol. 289, no. 3, F489–F495, 2005, PMID: 16093424. DOI: 10.1152/ajprenal.00467.2004. eprint: <http://www.physiology.org/doi/pdf/10.1152/ajprenal.00467.2004>. [Online]. Available: <http://www.physiology.org/doi/abs/10.1152/ajprenal.00467.2004>.
- [7] A. A. Karl-Erik Andersson, “Urinary bladder contraction and relaxation: Physiology and pathophysiology”, *Physiological Reviews*, vol. 84, no. 3, pp. 935–986, 2004, PMID: 15269341. DOI: 10.1152/physrev.00038.2003. eprint: <http://www.physiology.org/doi/pdf/10.1152/physrev.00038.2003>. [Online]. Available: <http://www.physiology.org/doi/abs/10.1152/physrev.00038.2003>.

- [8] G. Apodaca, “The uroepithelium: Not just a passive barrier”, *Traffic*, vol. 5, no. 3, pp. 117–128, 2004. DOI: 10.1046/j.1600-0854.2003.00156.x. [Online]. Available: <http://dx.doi.org/10.1046/j.1600-0854.2003.00156.x>.
- [9] S. N. A. Puneet Khandelwal and G. Apodaca, “Cell biology and physiology of the uroepithelium”, *American Journal of Physiology-Renal Physiology*, vol. 297, no. 6, F1477–F1501, 2009, PMID: 19587142. DOI: 10.1152/ajprenal.00327.2009. eprint: <http://www.physiology.org/doi/pdf/10.1152/ajprenal.00327.2009>. [Online]. Available: <http://www.physiology.org/doi/abs/10.1152/ajprenal.00327.2009>.
- [10] S. A. Lewis, “Everything you wanted to know about the bladder epithelium but were afraid to ask”, *American Journal of Physiology-Renal Physiology*, vol. 278, no. 6, F867–F874, 2000, PMID: 10836974. DOI: 10.1152/ajprenal.2000.278.6.F867. eprint: <https://doi.org/10.1152/ajprenal.2000.278.6.F867>. [Online]. Available: <https://doi.org/10.1152/ajprenal.2000.278.6.F867>.
- [11] H. J. L. W. R. Cross I. Eardley and J. Southgate, “A biomimetic tissue from cultured normal human urothelial cells: Analysis of physiological function”, *American Journal of Physiology-Renal Physiology*, vol. 289, no. 2, F459–F468, 2005, PMID: 15784840. DOI: 10.1152/ajprenal.00040.2005. eprint: <http://www.physiology.org/doi/pdf/10.1152/ajprenal.00040.2005>. [Online]. Available: <http://www.physiology.org/doi/abs/10.1152/ajprenal.00040.2005>.
- [12] [Online]. Available: <http://www.compucell3d.org/>.
- [13] M. H. Swat, J. Belmonte, R. W. Heiland, B. L. Zaitlen, J. A. Glazier, and A. Shirinifard, *Introduction to compucell3d v3.7.4*, 2017. [Online]. Available: www.compucell3d.org/BinDoc/cc3d_binaries/Manuals/Introduction_To_CompuCell3D_v.3.7.4.pdf.
- [14] J. A. Glazier, A. Balter, and N. Poplawski, “Magnetization to morphogenesis: A brief history of the glazier-graner-hogeweg model”, *Single-Cell-Based Models in Biology and Medicine*, p. 79, 2007. [Online]. Available: https://www.researchgate.net/profile/Ariel_Balter/publication/227073495_Magnetization_to_Morphogenesis_A_Brief_History_of_the_Glazier-Graner-Hogeweg_Model/links/00b7d52d79e94eadc7000000.pdf.
- [15] F. Graner and J. A. Glazier, “Simulation of biological cell sorting using a two-dimensional extended potts model”, *Phys. Rev. Lett.*, vol. 69, pp. 2013–2016, 13 Sep. 1992. DOI: 10.1103/PhysRevLett.69.2013. [Online]. Available: <https://link.aps.org/doi/10.1103/PhysRevLett.69.2013>.

- [16] J. A. Glazier and F. Graner, “Simulation of the differential adhesion driven rearrangement of biological cells”, *Phys. Rev. E*, vol. 47, pp. 2128–2154, 3 Mar. 1993. DOI: 10.1103/PhysRevE.47.2128. [Online]. Available: <https://link.aps.org/doi/10.1103/PhysRevE.47.2128>.
- [17] E. Stott, N. Britton, J. Glazier, and M. Zajac, “Stochastic simulation of benign avascular tumour growth using the potts model”, *Mathematical and Computer Modelling*, vol. 30, no. 5, pp. 183–198, 1999. DOI: [https://doi.org/10.1016/S0895-7177\(99\)00156-9](https://doi.org/10.1016/S0895-7177(99)00156-9).
- [18] N. Chen, J. A. Glazier, J. A. Izaguirre, and M. S. Alber, “A parallel implementation of the cellular potts model for simulation of cell-based morphogenesis”, *Computer Physics Communications*, vol. 176, no. 11, pp. 670–681, 2007. DOI: <https://doi.org/10.1016/j.cpc.2007.03.007>.
- [19] T. M. Cickovski, C. Huang, R. Chaturvedi, T. Glimm, H. G. E. Hentschel, M. S. Alber, J. A. Glazier, S. A. Newman, and J. A. Izaguirre, “A framework for three-dimensional simulation of morphogenesis”, *IEEE/ACM Transactions on Computational Biology and Bioinformatics*, vol. 2, no. 4, pp. 273–288, Oct. 2005. DOI: 10.1109/TCBB.2005.46.
- [20] A. Torelli, P. Erben, J. Debatin, and M. Gumbel, “Proliferation and regeneration of the healthy human urothelium: A multi-scale simulation approach with 16 hypotheses of cell differentiation”.
- [21] A. Torelli, “Computer simulation of urothelial cells”, Master’s thesis, Mannheim, University of Applied Sciences, 2014.
- [22] B. K. P. Horn, “Extended gaussian images”, *Proceedings of the IEEE*, vol. 72, no. 12, pp. 1671–1686, Dec. 1984. DOI: 10.1109/PROC.1984.13073.
- [23] [Online]. Available: <http://mathworld.wolfram.com/RhombicDodecahedron.html>.
- [24] K. Meyer, O. Ostrenko, G. Bourantas, H. Morales-Navarrete, N. Porat-Shliom, F. Segovia-Miranda, H. Nonaka, A. Ghaemi, J.-M. Verbavatz, L. Brusch, I. Sbalzarini, Y. Kalaidzidis, R. Weigert, and M. Zerial, “A predictive 3d multi-scale model of biliary fluid dynamics in the liver lobule”, *Cell Systems*, vol. 4, no. 3, 277–290.e9, 2017/03/22 2017. DOI: 10.1016/j.cels.2017.02.008.
- [25] S. Kang, S. Kahan, J. McDermott, N. Flann, and I. Shmulevich, “Biocellion : Accelerating computer simulation of multicellular biological system models”, *Bioinformatics*, vol. 30, no. 21, pp. 3101–3108, 2014. DOI: 10.1093/bioinformatics/btu498. eprint:

/oup/backfile/content_public/journal/bioinformatics/30/21/10.1093_bioinformatics_btu498/2/btu498.pdf.

- [26] F. P. Cercato, J. C. M. Mombach, and G. G. H. Cavaleiro, “High performance simulations of the cellular potts model”, in *20th International Symposium on High-Performance Computing in an Advanced Collaborative Environment (HPCS’06)*, May 2006, pp. 28–28. DOI: 10.1109/HPCS.2006.28.